Chaos-assisted tunneling

Steven Tomsovic*
Department of Physics, FM-15 University of Washington, Seattle, Washington 98195
Denis Ullmo
Division de Physique Théorique, Institut de Physique Nucléaire, 91406 Orsay Cedex, France
(Received 20 August 1993)

We discuss and give evidence for the existence of a new mechanism for quantum dynamical tunneling. It may occur when a quantum system's underlying classical dynamics are far from integrability. In these circumstances, we show that the dominant tunneling contributions arise through chaos-assisted processes. This leads to behavior that is drastically different from that found in integrable and quasi-integrable systems. In particular, one can observe a marked crossing mechanism when a chaotic level passes nearby the tunneling ones, and the distributions of splitting (due to tunneling) can be modeled using properly designed ensembles of random matrices. Such tunneling should be amenable to experimental detection.

PACS number(s): 05.45.+b, 03.65.Sq, 05.40.+j

I. INTRODUCTION

Tunneling may be defined as a quantum mechanical manifestation of a classically forbidden process, taking for granted that there exists a well defined classical analog of the quantum system of interest. Two paradigms in one-degree-of-freedom (1d) systems are the transmission through potential step barriers and the small energy splittings within pairs of symmetric and antisymmetric eigenstates of the double well potential. In these cases, tunneling occurs in the sense that classical trajectories remain on one side of a potential barrier whereas quantum mechanically it is possible to go through. As for many 1d isolated, conservative, tunneling systems, the magnitude of such effects have long been well understood and are derivable in a number of ways.

In multiple-degree-of-freedom systems, the subject is much less advanced in understanding and suffers from a number of complications. An important warning sign that this might be the case starts with the recognition that the very nature of classical dynamics itself is far more diverse in its realm of possibilities, i.e., regular motion, chaotic motion, or the two intimately intertwined. Even in the relatively simpler case of integrable dynamics, tunneling is not yet fully understood in spite of a long history and some very promising recent works [1,2]. The explanation, in a sense, lies in the fact that multidimensional tunneling is a far richer phenomenon. To start with, a potential barrier is no longer needed in order to split or divide the phase space. In integrable systems, for instance, almost all trajectories are trapped on d-dimensional surfaces in the $2d$-dimensional phase space (invariant tori). A certain subset of these invariant tori provides the support for a semiclassical quantization of the system through Einstein-Brillouin-Keller (EBK) theory [3]. The Kol'mogorov-Arnol'd-Moser (KAM) theorem [4] ensures that if the integrability is slightly broken, most of the invariant tori remain, albeit distorted and embedded in an intricate background of feeble resonances and chaotic motion. A generalized tunneling may then occur between tori whether or not the perturbation gave rise to a potential barrier. In addition, tunneling may also be important at all energies since the trapping of classical motion is not restricted to occurring below some barrier.

The generic dynamics for few-degree-of-freedom systems is really the mixed case for which the phase space is shared between "chaotic seas" containing no invariant tori and "regular islands" filled densely with invariant tori. In a semiclassical treatment, a special role is played by the tori fulfilling the EBK quantization conditions

$$J_i = 2\pi\hbar\left(n_i + \frac{\nu_i}{4}\right) \qquad (i = 1, \ldots, d), \tag{1}$$

where the

$$J_i = \oint_{C_i} \mathbf{p}\, d\mathbf{q} \tag{2}$$

are the action integrals taken on d independent closed paths C_i on the torus. The Maslov indices ν_i are integers which count the number of caustics encountered by the C_i. To each of these quantizing tori, what has been termed a "quasimode" by Arnold [5] can be associated. That is a quantum wave function which fulfills the Schrödinger equation to any order in $\hbar$; see, for instance, Maslov [6]. These quasimodes are in general also good approximations of the actual wave functions, but in some cases, as for the double well system, the exact eigenfunctions are actually linear combinations of two (or more) quasimodes quantizing at or near the same energy. As a consequence, a quasimode constructed on a given torus may after a very long time evolve onto another torus, despite the classical trajectory being indefinitely trapped on the original one. This effect has been dubbed "dynamical" tunneling by Davis and Heller [7]. It frequently occurs in simple systems such as models of the nuclear

*Permanent address: Department of Physics, Washington State University, Pullman, WA 99164.

motion of small molecules [8].

Another point which makes the tunneling in multiple-degree-of-freedom systems (or time-dependent 1d systems [9]) richer is the possible coexistence mentioned above of chaos and regular motion. Our aim in this paper is to show that in this mixed phase space situation a new tunneling mechanism exists in which chaos-assisted processes dominate. Indeed, in the treatment of 1d tunneling as well as multidimensional tunneling for (nearly) integrable systems, the two quasimodes at or near the same energy are rightfully treated as an isolated system. We shall see that in the presence of chaos, the influence of the neighboring chaotic states, which encompass all the complexity of the classical motion in the chaotic region, cannot, in general, be ignored. This leads to much larger and erratic tunneling rates without a simple identifiable dependence on $\hbar$ and causes a great sensitivity to the variation of an external parameter. In particular, there will be a characteristic "crossing mechanism" as a chaotic level passes by the regular ones with the parameter's variation. In this simple case, the tunneling process is a three level problem. If no chaotic state plays a predominant role, one faces a multilevel mechanism. We shall show that a correct description of the statistical properties of the tunneling can be modeled with an ensemble of random matrices. The resulting Gaussian ensembles describing the chaotic levels are based on those used to interpret the spectral fluctuations of mixed phase space systems [10]. The good agreement between the predicted and observed splitting distribution is another manifestation of the major role played by the surrounding chaotic motion in the tunneling process. It will be seen that it is necessary to understand the magnitude of the mean square tunneling matrix elements and the transport properties inside the chaotic regions (i.e., how quickly a typical classical trajectory goes from the neighborhood of a tunneling torus to that of its twin partner) in order to predict the splitting distributions. This is consistent with the observation made by Bohigas *et al.* [11] on the bicircular billiard.

Before entering the heart of the topic we shall present a slightly different procedure for calculating the tunneling splitting in the double well which will have the advantage of emphasizing its two-level character. We will then make a comparison with what would be expected if a third state were to enter the problem. The system of two coupled quartic oscillators with a mixed dynamics will be investigated. The tunneling behavior will then be shown to be incompatible with the usual two-level treatment, but to fit well with the multilevel one. This will stress the major role played by the surrounding chaotic dynamics.

II. ISOLATED vs EMBEDDED TUNNELING DOUBLETS

A. The double well revisited: Isolated doublets

To begin, we redo the standard calculation of the splitting in the symmetric double well because it is important for our purposes to manifest explicitly the reduction to a two level (isolated doublet) system. Other approaches may lead to more compact, more familiar discussion, but they also, at least implicitly, depend on the isolated doublet image. Consider

$$H(p,q) = \frac{p^2}{2m} + V(q), \qquad V(q) = \alpha(q^2 - q_0^2)^2 \qquad (\alpha > 0)\,, \tag{3}$$

where p stands for $-i\hbar\partial/\partial q$ in the quantum version. For a given energy E, we shall in the following denote by $p(q)$ the two valued function

$$p(q) = \pm\sqrt{2m[E - V(q)]}, \tag{4}$$

where the sign ambiguity will not matter [note that $p(q)$ is complex when $E < V(q)$], and use $|p(q)|$ where we need to be more specific.

For $E < \alpha q_0^4$, the classical motion is confined in one of the two wells, q being in the range $[x_1, x_2]$ or $[-x_2, -x_1]$ with $x_1 = (q_0^2 - \sqrt{E/\alpha})^{1/2}$ and $x_2 = (q_0^2 + \sqrt{E/\alpha})^{1/2}$; see Fig. 1. To each energy E fulfilling the EBK quantization condition

$$\oint p(q)dq = 2\int_{x_1}^{x_2} |p(q)|dq = 2\pi\hbar(n + \tfrac{1}{2}) \tag{5}$$

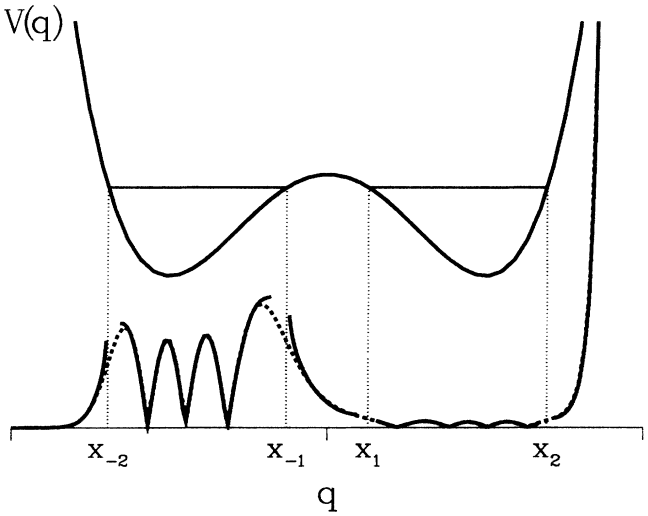

FIG. 1. Illustration of the double well and of the semiclassical solution of the corresponding Schrödinger equation. The upper part of the figure shows the double well potential of Eq. (3), the semiclassical energy E_3 obtained using the EBK quantization condition Eq. (5) for $n = 3$ ($\alpha = m = 1$ and $\hbar = 0.1$), and the corresponding classical turning points which are projected down by the dotted lines to the absolute values of the wave functions. The solid line is the semiclassical solution $\tilde{\Psi}_l$ given in Table I. There are gaps near the turning points where the approximation tends to infinity. The heavy dotted curve is the corresponding exact (non-normalizable) solution of the Schrödinger equation.

or

$$\oint p(q)dq = 2\int_{-x_2}^{-x_1} |p(q)|dq = 2\pi\hbar(n+\tfrac{1}{2})$$

can be associated two quasimodes $\tilde{\Psi}_l$ and $\tilde{\Psi}_r$ living, respectively, in the left and right wells. Let us consider more carefully why they are not actual eigenfunctions of the quantum operator $\hat{H}$. In the classically allowed regions (i.e., $q \in [x_1, x_2]$ for $\tilde{\Psi}_r$, $q \in [-x_2, -x_1]$ for $\tilde{\Psi}_l$) and sufficiently far from the turning points, $\pm x_1$, $\pm x_2$, $\tilde{\Psi}_l$, and $\tilde{\Psi}_r$ are given by

$$\tilde{\Psi}_r = a(q)\cos\left(\frac{1}{\hbar}\int_{x_1}^{q}|p(q)|\,dq - \frac{\pi}{4}\right) \quad (\text{for } q \in [x_1, x_2]) \tag{6}$$

$$\tilde{\Psi}_l = a(q)\cos\left(\frac{1}{\hbar}\int_{-x_1}^{q}|p(q)|\,dq + \frac{\pi}{4}\right)$$

$$(\text{for } q \in [-x_2, -x_1])\,,$$

where

$$a(q) = \sqrt{\frac{\omega}{2\pi|p(q)|}}\,, \tag{7}$$

with ω the angular frequency of the trajectory. They can be continued outside their respective allowed region in such a way that they fulfill (in the semiclassical approximation) the Schrödinger equation on the whole real axis. Let us introduce $S(q)$ the action function defined by

$$S(q) = \int^{q} p(q)\,dq\,. \tag{8}$$

An additive constant is of no importance here so we omit the lower bound of integration, but $S(q)$, as $p(q)$, should be considered as a two valued function. Using the fact that between each turning point the semiclassical approximations of the Schrödinger equation are linear combinations of the two functions

$$\frac{1}{\sqrt{|p(q)|}}\exp\left(\frac{i}{\hbar}S(q)\right) \tag{9}$$

corresponding to the two possible values of S, together with the Langer connection formula [12] (which we recall in Appendix A), one obtains, far from the turning points, the "semiclassical" solutions of the Schrödinger equation. The continuation of Eq. (6) is given in Table I where

$$\xi = \int_{-x_1}^{+x_1}|p(q)|\,dq \tag{10}$$

is the action integral taken between the two turning points $\pm x_1$. A comparison between such a semiclassical solution of the Schrödinger equation and the corresponding exact one is displayed in Fig. 1. $\tilde{\Psi}_r$ and $\tilde{\Psi}_l$ defined in this way are, however, not proper wave functions since they are not normalizable. $\tilde{\Psi}_l$, for instance, grows exponentially when q is greater than x_2. To remain in the quantum Hilbert space, one must therefore eliminate this behavior in some way, for instance, by multiplying $\tilde{\Psi}_l$ by some function $\varphi_l(q)$ such that

$$\varphi_l(q) = \begin{cases} 1 \text{ for } q < 0 \\ 0 \text{ for } q > x_1 \end{cases} \tag{11}$$

and $\varphi_l(q)$ decreases smoothly in the range $0 < q < x_1$. Defining in the same way $\varphi_r(q) = \varphi_l(-q)$, the functions

$$\Psi_l = \varphi_l(q)\tilde{\Psi}_l, \quad \Psi_r = \varphi_r(q)\tilde{\Psi}_r \tag{12}$$

are now proper (normalized) quantum states, but no longer solutions of the Schrödinger equation. One can, however, use a simple form of Maslov's commutation formula 8.5 [6], which in our case states that for any smooth function φ one has in the semiclassical approximation

$$(\hat{H}-E)\varphi(q)\frac{e^{iS(q)/\hbar}}{\sqrt{|p(q)|}} = -i\hbar\frac{p}{m}\frac{d\varphi}{dq}\frac{e^{iS(q)/\hbar}}{\sqrt{|p(q)|}} \tag{13}$$

[$S(q)$ is the action function defined in Eq. (8)]. For the matrix element ϵ connecting Ψ_l and Ψ_r, this leads to

TABLE I. Semiclassical solutions of the Schrödinger equation associated with the Hamiltonian of Eq. (3). The wave functions $\tilde{\Psi}_l$ and $\tilde{\Psi}_r$ continue (using the Langer connection formula given in Appendix A) along the whole real axis with the semiclassical approximations of Eq. (6) defined, respectively, in the left and right wells. $a(q)$ is given by Eq. (7) and ξ by Eq. (10). See Fig. 1.

	$\tilde{\Psi}_l$	$\tilde{\Psi}_r$
$-\infty < q < -x_2$	$\frac{a(q)}{2}\exp\left(\frac{1}{\hbar}\int_{-x_2}^{q}\lvert p(q)\rvert\,dq\right)$	$e^{-\frac{\xi}{\hbar}}\frac{a(q)}{2}\exp\left(\frac{1}{\hbar}\int_{-x_2}^{q}\lvert p(q)\rvert\,dq\right)$
$-x_2 < q < -x_1$	$a(q)\cos\left(\frac{1}{\hbar}\int_{-x_1}^{q}\lvert p(q)\rvert\,dq + \frac{\pi}{4}\right)$	$e^{-\frac{\xi}{\hbar}}\frac{a(q)}{2}\cos\left(\frac{1}{\hbar}\int_{-x_1}^{q}\lvert p(q)\rvert\,dq - \frac{\pi}{4}\right)$
$-x_1 < q < x_1$	$\frac{a(q)}{2}\exp\left(-\frac{1}{\hbar}\int_{-x_1}^{q}\lvert p(q)\rvert\,dq\right)$	$\frac{a(q)}{2}\exp\left(-\frac{1}{\hbar}\int_{x_1}^{q}\lvert p(q)\rvert\,dq\right)$
$x_1 < q < x_2$	$e^{-\frac{\xi}{\hbar}}\frac{a(q)}{2}\cos\left(\frac{1}{\hbar}\int_{x_1}^{q}\lvert p(q)\rvert\,dq + \frac{\pi}{4}\right)$	$a(q)\cos\left(\frac{1}{\hbar}\int_{x_1}^{q}\lvert p(q)\rvert\,dq - \frac{\pi}{4}\right)$
$x_2 < q < +\infty$	$e^{-\frac{\xi}{\hbar}}\frac{a(q)}{2}\exp\left(\frac{1}{\hbar}\int_{x_2}^{q}\lvert p(q)\rvert\,dq\right)$	$\frac{a(q)}{2}\exp\left(\frac{1}{\hbar}\int_{x_2}^{q}\lvert p(q)\rvert\,dq\right)$

$$\epsilon = \langle \Psi_l | \hat{H} | \Psi_r \rangle = \int dq\, \tilde{\Psi}_l^* \tilde{\Psi}_r \left| \frac{d\varphi_s}{dq} \right| \frac{\hbar |p|}{m} \quad (s = l \text{ or } r) \,. \tag{14}$$

Noting that $\tilde{\Psi}_l^* \tilde{\Psi}_r |p|$ is independent of q and equal to $\omega \exp(-\xi/\hbar)/8\pi$ in the support of $d\varphi_s/dq$, one finally obtains

$$\epsilon = \frac{\hbar\omega}{8\pi m} \exp(-\xi/\hbar) \,, \tag{15}$$

which is independent of the precise choice made for φ_l and φ_r. [In fact, one can check easily that φ_l and φ_r can be chosen with even fewer constraints than we imposed. For instance, one may allow $0 < \varphi_l < 1$ in the range $x_1 < q < x_2$ without changing Eq. (15).]

The actual eigenfunctions

$$\Psi_+ = \frac{1}{\sqrt{2}} (\Psi_l + \Psi_r) \,, \quad \Psi_- = \frac{1}{\sqrt{2}} (\Psi_l - \Psi_r) \tag{16}$$

and the tunneling splitting $\Delta E = 2\epsilon$ are thus simply obtained by projecting the Hamiltonian on the two-dimensional space $\Psi_l \oplus \Psi_r$, generated by Ψ_l and Ψ_r, and diagonalizing the two by two matrix $\tilde{H}_2$ ($\equiv \hat{H}$ projected on $\Psi_l \oplus \Psi_r$),

$$\tilde{H}_2 \begin{pmatrix} \Psi_l \\ \Psi_r \end{pmatrix} = \begin{pmatrix} E & \epsilon \\ \epsilon & E \end{pmatrix} \begin{pmatrix} \Psi_l \\ \Psi_r \end{pmatrix} \,. \tag{17}$$

B. The three-level mechanism: Embedded doublets

The usual (regular) tunneling can be referred to as a "two-level mechanism" due to the fact that all the tunneling information is contained in Eq. (17). It might occur, and we shall see that it does when mixed dynamics is involved, that some other nondegenerate state Φ_+^c, say, of the same symmetry as Ψ_+, interacts sufficiently with Ψ_+ that it cannot be neglected. We suppose here that, as for the double well considered above and the quartic oscillators which we shall study in Sec. III, the eigenfunctions are classified into symmetry classes. It is an important point that there is no corresponding Φ_-^c (Φ_+^c is not part of a doublet). Denoting v the matrix element connecting Ψ_+ and Φ_+^c, and E^c the mean energy of the latter, one can rightfully see that even if the direct coupling ϵ were to vanish (i.e., $\epsilon \ll v^2/|E^c - E^r|$), indirect tunneling occurs between the two quasimodes Ψ_l and Ψ_r. Indeed, with $\epsilon \to 0$, the Hamiltonian $\hat{H}$ projected on the three-dimensional space generated by Ψ_l, Ψ_r, and Φ_+^c, has the following simple form in the symmetrized basis:

$$\tilde{H}_3 \begin{pmatrix} \Psi_- \\ \Psi_+ \\ \Phi_+^c \end{pmatrix} = \begin{pmatrix} E^r & 0 & 0 \\ 0 & E^r & v \\ 0 & v & E^c \end{pmatrix} \begin{pmatrix} \Psi_- \\ \Psi_+ \\ \Phi_+^c \end{pmatrix} \,. \tag{18}$$

For convenience, assume v^2 is still sufficiently small that $v^2 \ll (E^c - E^r)^2$. One finds a splitting $\chi = v^2/|E^c - E^r|$ between the two quasidegenerate eigenvalues. Obtaining the time evolution of, say, Ψ_l, is also immediate: under the action of $\hat{U}(t) = \exp(-i\hat{H}t/\hbar)$, the antisymmetric component just picks up a phase $\exp(-iE^r t/\hbar)$ and the propagation of the symmetric, regular component follows from the standard treatment of the two-level problem. There will be a weak oscillation of probability amplitude transfer from Ψ_+ to Φ_+^c and back of magnitude $b[\approx |v/(E^c - E^r)|]$ and period t_0 $[\approx 2\pi\hbar/|E^c - E^r|]$. At the end of each period, $\hat{U}(t_0)\Psi_+$ results in just an acquired overall phase $\exp[-i(E^r - \chi)t_0/\hbar]$ where, relative to $U(t_0)\Psi^-$, there is an extra phase fixed by χ. Thus after n periods,

$$\hat{U}(nt_0)\Psi_l = e^{-iE^r nt_0/\hbar} \left(\Psi_- + e^{i\chi nt_0/\hbar} \Psi_+ \right) \,. \tag{19}$$

As the relative dephasing of Ψ_+ and Ψ_- increases with time, the initial state is resonantly tunneling back and forth between Ψ_l and Ψ_r without ever fully appearing on Φ_+^c. The image is that during each time step t_0, a small piece of one quasimode breaks off and is transferred to Φ_+^c. By the end of the period t_0, that small piece has moved onto the symmetric partner quasimode. The total elapsed time to tunnel completely from one quasimode to another is $\pi/\chi \simeq t_0/2b^2$, which is just a simple combination of the squared amplitude and oscillation period.

The Hamiltonian, Eq. (18), thus describes a tunneling process. However, the embedded doublet will have some fundamental differences with respect to the isolated doublets. The most fundamental distinction concerns the behavior of the tunneling rate under the variation of an external parameter λ. Indeed, one expects a smooth behavior of the splittings in the two-level case, whereas in the three-level case there will be a marked crossing mechanism as the two lines $E^c(\lambda)$ and $E^r(\lambda)$ approach each other which will translate into a large enhancement of the tunneling rate. The tunneling behavior overall will be very erratic. It will be seen in the following section, with the example of a system of two coupled quartic oscillators, that the tunneling process for sufficiently nonintegrable dynamics cannot be accounted for by the isolated doublet mechanism. There will exist diabatic states not associated with any regular motion that play an essential role. The morphology of these "chaotic" states is quite different from the quasimodes (quantized tori), which are much more localized in a phase space sense. When a chaotic state lies close in energy to a regular doublet, it will be shown that the three-level mechanism applies, with Ψ_- and Ψ_+ being regular states constructed on symmetric invariant tori and Φ_+^c a chaotic state. The resultant splitting distributions cannot be confused with what is observed for regular systems.

III. TUNNELING IN A MIXED SYSTEM

Before continuing with a more elaborate modeling of chaos-assisted tunneling, it is worth first examining an explicit example in order to demonstrate its presence and key features. A system of two coupled quartic oscillators provides an excellent realization [10]. They are governed by the Hamiltonian

$$H = \mathbf{p}^2/2 + V(\mathbf{q}),$$
$$V(\mathbf{q}) = a(\lambda)\left(q_1^4/b + bq_2^4 + 2\lambda q_1^2 q_2^2\right). \tag{20}$$

λ specifies the coupling of the two modes, $b \neq 1$ lowers the symmetry from that of a square to a rectangle (in practice we take $b = \pi/4$), and $a(\lambda)$ is an adjustable constant used in simplifying the quantum calculations. This system is quite ideal in many respects for a study of chaos and tunneling. By varying λ from 0 to -1 we can select the desired degree of chaos since the system is integrable (separable) for $\lambda = 0$ and is essentially chaotic for $\lambda = -1$. The homogeneous nature of the potential both simplifies the quantum and classical calculations as well as the ensuing interpretations of the semiclassical mechanics. The classical study is performed on the energy surface $E = 1$ and the dynamics on any other surface is obtained through a simple rescaling.

Quantum mechanically we may solve Schrödinger's equation in two different ways that in this case are equivalent to within a rescaling. One can either solve it in the standard way for the quantizing energies $\{E_j\}$ or fix $E = 1$ and solve for the quantizing values of Planck's constant $\{\hbar_j\}$. In fact, with our choice of $a(\lambda)$, it is true both that $\{E_j^{3/4}\} = \{\hbar_j^{-1}\}$ and that the Thomas-Fermi term of the level density is independent of λ. $[a(\lambda)^{1/2} = 2mK[(1-\lambda)/2]/3\pi\hbar^2$, where $K(z)$ is a complete elliptic integral of the first kind; see [10].] Even though the quantum solutions are actually found in the usual way, it is perfectly justified maintaining that we are working quantum mechanically (and classically) at $E = 1$ and with $\hbar \to 0$ in moving up the spectrum. We shall stress the $\hbar$ dependence by continuing with this viewpoint. With a little effort we were able to calculate up to the first $\sim 30\,000$ eigenvalues for interesting values of (λ, b) so that $\hbar$ is approximately 170 times smaller at the top of the spectra as compared with the ground states. The precision of the levels is good to approximately $10^{-5} - 10^{-6}$ of a mean spacing. The details of the numerical computations can be found in [10].

A useful way to study the classical dynamics is through the construction of surfaces of section. Here we follow trajectories and record their phase space coordinates (q_2, p_2) every time they cross the $q_1 = 0$ plane with positive momentum p_1. The invariant tori appear as simple closed curves and the chaotic regions appear as filled in black areas outlining the impenetrable KAM islands. Figure 2 illustrates a section for one value of the coupling λ ($\lambda = -0.25$). In the same way as in the double well system, the trajectories belonging to island $1a$ are symmetric but distinct from those belonging to island $1b$; see Fig. 3. Thus, to each torus in the upper island which fulfills the EBK quantization conditions, Eq. (1) ($d = 2$, $\nu_1 = 2$, and $\nu_2 = 4$), corresponds a twin symmetric partner which also satisfies them. For a significant range of the parameter λ ($\lambda \in [-1, \lambda^*]$, $\lambda^* \simeq -0.20$), a similar behavior occurs for all the other regular islands. It implies that, to the EBK approximation and in this range of λ, all the regular levels occur in degenerate pairs with different reflection symmetries $(\epsilon_1, \epsilon_2) = (\pm, \pm)$ (ϵ_i associated with $\hat{P}_i$: $q_i \longrightarrow -q_i$, $p_i \longrightarrow -p_i$, $i = 1, 2$), as dictated by the symmetry of these islands. On the contrary, the dominant chaotic region (the majority of the phase space) does not have a symmetric but distinct corresponding partner region. It is invariant under reflection and no quasidegeneracies are expected for the chaotic states [13]. This makes it possible (see [14,10]) to perform in a simple yet clear fashion the separation in the quantum spectrum between the regular levels (those asso-

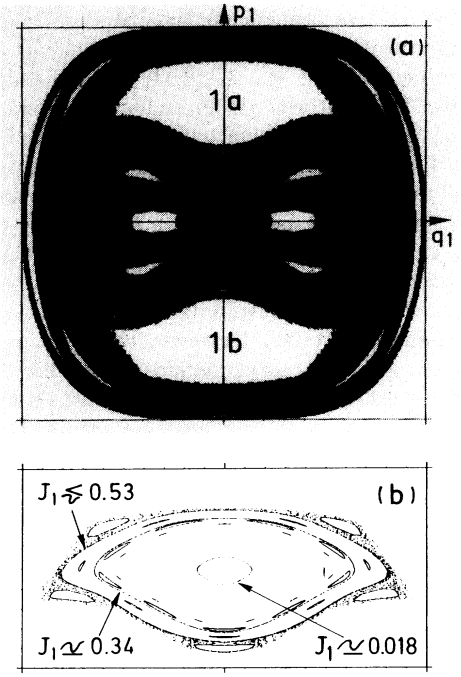

FIG. 2. (a) $q_2 = 0$ surface of section for $\{(\lambda, b) = (-0.25, \pi/4)\}$. The blackened region is a single connected zone of chaotic motion. The KAM regions are the open areas. The large islands, denoted $1a$ and $1b$, are part of a 1:1 resonance island chain and are symmetric versions of each other. (b) The island $1a$ magnified. Included are the tori with (at $E = 1$) $J_1 = 0.018$ (the smallest to quantize in our spectrum), $J_1 = 0.34$, and $J_1 = 0.53$; see Fig. 4.

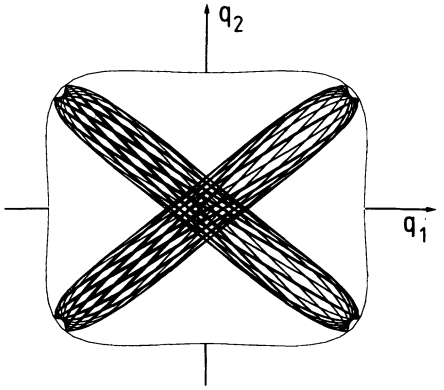

FIG. 3. Configuration space drawing of symmetry related tori from islands $1a$ and $1b$ for $\{(\lambda, b) = (-0.25, \pi/4)\}$. The outline is the equipotential curve.

ciated with an invariant torus) and the chaotic ones (the remaining states). Quantum numbers (n_1, n_2) can also be determined so that via the EBK quantization conditions of Eq. (1) the torus associated with a given regular state is entirely specified. For island 1 of the case displayed in Fig. 2, the maxima n_1 and n_2 in the spectrum we calculate are approximately 20 and 265, respectively.

In practice, the regular levels are not exactly degenerate since tunneling takes place between the quasimodes constructed on symmetric tori. Very little practical theory exists concerning the evaluation of the direct coupling in more than 1d systems. However, the work of Wilkinson [1] gives a satisfactory description, which although derived for a limited class of Hamiltonians, its main features should be relevant on a more general footing. The main point we shall retain is that, to leading order, the splitting ΔE_d due to the direct coupling ϵ is given by an expression such as,

$$\Delta E_d = A e^{-\xi/\hbar}, \tag{21}$$

where, as in Eq. (15), A has a smooth behavior in $\hbar$ and ξ is the imaginary part of an action integral taken on a complex path. In other words, ξ is a purely classical quantity and if one is able to tune $\hbar$ and to observe the splitting between states constructed on exactly the same tori, the data should gently fall on a line of slope -1 in a $\log_{10} \Delta E$ vs $1/\hbar$ plot. This has been done explicitly and verified by Wilkinson for some nearly integrable systems [15].

With the quartic oscillators, one can in the same manner take advantage of the homogeneity of the potential to obtain a tuning of $\hbar$. Indeed, those tori which are quantizing are doing so for an infinite set of quantum numbers (assuming one fixes the energy to $E = 1$ and looks for the quantizing values of $\hbar$). One may thus observe how the splitting changes keeping the classical mechanics strictly identical but for different values of $(n_1 + 1/2)$, which plays the role of $1/\hbar$. Figure 4 shows the results obtained for a set of three tori from the $(-0.25, \pi/4)$ case. For each of them there exist fluctuations of several orders of magnitude. A simple $\hbar$ dependence such as Eq. (21) is excluded. Nor does any obvious indication of predictable dependence on $\hbar$ exist. It is impossible for this behavior to be interpreted in terms of a two-level mechanism if A and ξ are to have a classical significance.

By observing the behavior of the splittings under variation of an external parameter (here the coupling constant λ), one can see that there is a crossover in the behavior from the two-level to multilevel mechanism where the system changes from having nearly integrable dynamics to mixed dynamics. Figure 5 illustrates, with surfaces of section, the changing dynamics as a function of λ. For $\lambda = 0$ (integrable), the invariant tori of the uncoupled quartic oscillators are symmetric under the action of $\hat{P}_1$ and $\hat{P}_2$ and their intersection with the Poincaré section appears as concentric closed curves centered around the origin. There is therefore no associated quasidegeneracies in the quantum spectrum; there may be close lying levels though from quantizing tori that happen to be close to satisfying a resonance condition. As λ decreases from zero, the system starts in the quasi-integrable regime,

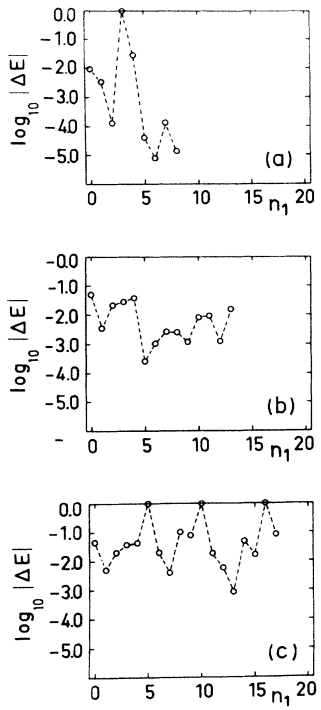

FIG. 4. Logarithm of the tunneling splittings, rescaled to unit mean spacing, for three tori versus n_1 $\{(\lambda, b) = (-0.25, \pi/4)\}$. n_1 plays the role of $\hbar^{-1}$. The points are connected by dashed lines for easier viewing. A zero value indicates that the pair could not be easily located. At $E = 1$, (a) torus $J_1 = 0.34$, (b) torus $J_1 = 0.53$, and (c) presumed cantorus $J_1 = 0.68$ just outside the KAM region and 2/5 resonance. Also given in Ref. [10].

the little chaos present is narrowly confined and develops only over long time scales. $\hbar$ in our spectra is much too large to detect that the system is nonintegrable and there are no irregular states forming yet, even though resonances are beginning to develop. In particular, the 1:1 resonance (islands $1a$ and $1b$) is large enough to quantize directly even for λ very close to zero. Therefore, the levels quantized in their interiors are becoming more and more degenerate under further perturbation as the resonances grow; this is an example of level attraction, so to speak [8]. The growth of islands 1 ceases for a value of λ near $\lambda^* \approx -0.20$ where the last original torus is destroyed. At this point the chaos is becoming pervasive and many irregular levels begin to exist; all the remaining tori now occur in pairs. Beyond λ^*, only one large chaotic region remains, the irregular levels take over as the overwhelming majority, and the islands begin to shrink, essentially disappearing for $\lambda \leq -0.5$.

In Fig. 6, we show the splittings for three tunneling pairs (associated with islands 1) as a function of λ from before the islands' creation ($\lambda = 0$) to well beyond their destruction ($\lambda = -0.60$). In so doing, the quantum numbers (n_1, n_2) are fixed for each level thus defining via Eq. (1) a one parameter family of tori. As desired, with the variation of λ, $\hbar$ changes little for a given level; in the figure the three levels shown are given in the order of

decreasing $\hbar$. One sees near $\lambda = 0$ the quasi-integrable regime where the splittings behave smoothly and they have no relation to the proximity of other levels; this confirms the same physics as the above mentioned Wilkinson calculation. A quasidegenerate pair is rightfully considered as an isolated two-level tunneling system and, not surprisingly, we find that the exponential $\hbar^{-1}$ dependence given in Eq. (21) is loosely verified. For example, compare Figs. 6(a) and 6(c), which were selected in order that they derive from the exact same family of tori. Their approximate factor 3 difference in the slopes of the initial roughly linear portion of the curves matches the factor 3 difference in $\hbar$ between their quantizations at any given value of λ.

Beyond the quasi-integrable regime, which shrinks with $\hbar$, the tunneling becomes sensitive to the nonintegrability of the system. It happens that under perturbation of the Hamiltonian, the quasidegenerate pairs cross the paths of other, mostly irregular levels; the number of crossings grows faster than the level density as $\hbar \to 0$ and could only be marked on Figs. 6(a) and 6(b).

It turns out that in the neighborhood of the crossing, the tunneling is actually described by the three-level mechanism of Eq. (18). Suppose that near the crossing point, $\Delta E \equiv E^c - E^r$ varies linearly with the coupling parameter λ, i.e., $\Delta E = c(\lambda - \lambda_0)$, and the tunneling matrix element is locally constant. The three parameters v (tunneling matrix element), λ_0 (crossing point), and c (slope of the crossing) can then be determined by any three values of the splitting $\delta(\lambda)$ corresponding to three values of the coupling near the crossing point. The parameters are extracted by inverting $\delta = \sqrt{\Delta E^2 + 4v^2} - \Delta E$ to its quadratic form and using its first two exact discrete derivatives. This is illustrated in Fig. 7 where the value of the deduced v is plotted directly below the local portion of the spectrum used in its extraction. The result is a plateau in the neighborhood of each crossing which confirms that the above picture of the isolated avoided level crossing is appropriate. The neighborhood of the peaks are thus clearly described by a three-level mechanism.

Unlike the quasi-integrable regime, crossings with chaotic levels here most of the time have a strong effect on the resultant splittings leading to the observed fluctuations and the direct tunneling component is orders of

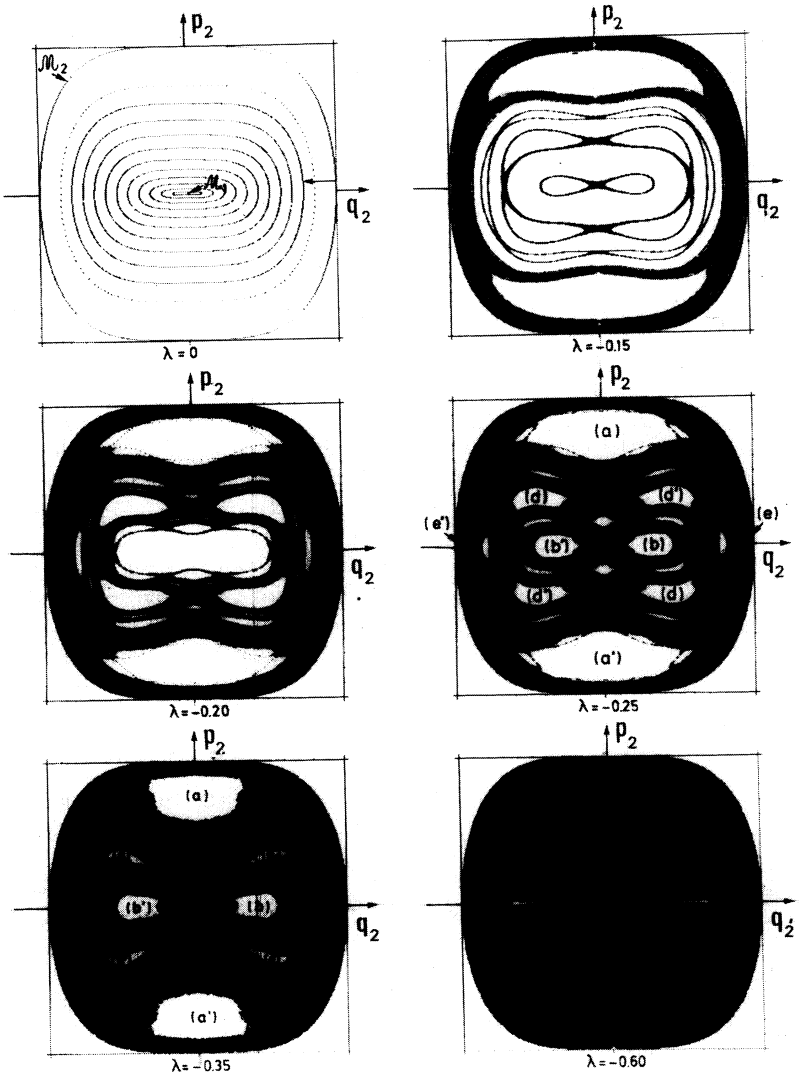

FIG. 5. $q_1 = 0$ surface of sections showing the changing dynamics with λ ($b = \pi/4$). The system becomes increasingly chaotic as λ decreases. Also given in Ref. [10].

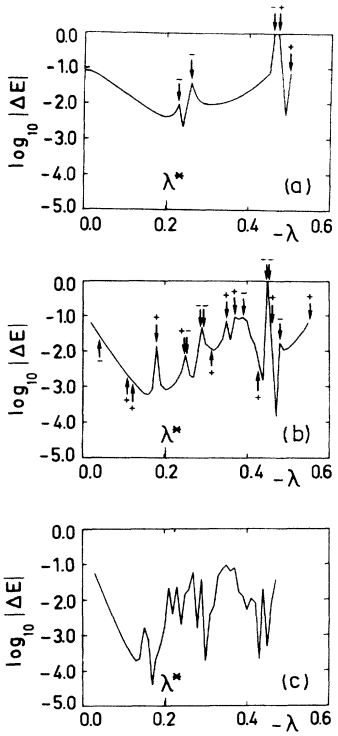

FIG. 6. Logarithm of the tunneling splittings, rescaled to unit mean spacing, for 3 cases of fixed quantum numbers (n_1, n_2) versus λ. $\hbar$ decreases by an exact factor 3 between (a) and (c). The arrows indicate the avoided level crossings, occurring (+) between the symmetry $(\epsilon_1, \epsilon_2) = (+,+)$ levels and $(-)$ between the $(-,-)$ ones. The (n_1, n_2) values are (a) (0,14), (b) (0,24), and (c) (1,44). Also given in Ref. [10].

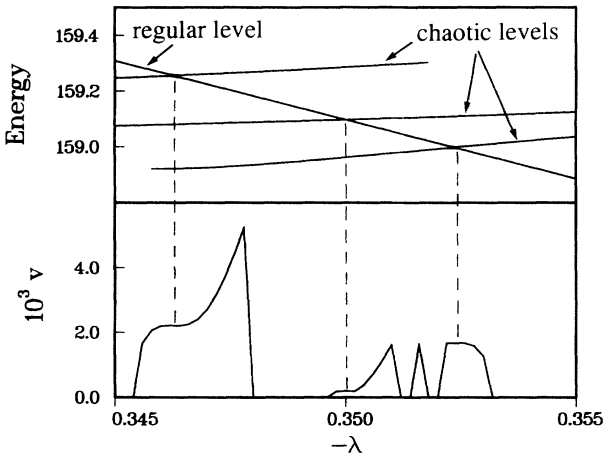

FIG. 7. Stability of the extraction of tunneling matrix elements. In the upper box a regular level (quantized torus) descends across the paths of many chaotic levels as λ varies over a narrow range. Shown in the lower box is the corresponding value of the tunneling matrix element extracted by the method discussed in the text. Near the avoided crossings the obtained value shows a plateau whereas otherwise it is erratic and often complex (put to zero in the figure). This illustrates the range over which the system locally behaves as described by the three-level mechanism. The avoided crossing points are projected down for easier visual alignment.

magnitude too feeble to be detected. On the contrary, it can be checked that crossing another regular state (which here means crossing another regular doublet) has little effect on the splittings. The predominance of the embedded doublet mechanism is therefore characteristic of the existence of a chaotic component in the phase space. In fact, a heuristic explanation of this behavior follows if one assumes that the connecting matrix element between a quasimode (such as the one constructed in Sec. II A) and another state decreases *exponentially* with the distance in "phase space" separating them. Quasimodes on which the tunneling states are constructed are localized on invariant tori that must lie far apart. Regular states are localized on invariant tori, which cannot be close to both tori on which the tunneling states are constructed. They are thus only very slightly connected to tunneling states. On the contrary a chaotic state is roughly speaking delocalized in the whole chaotic region and thus (see again Fig. 2) is in contact with both islands to which the tunneling states belong. Its distance from the tori on which the tunneling states are built is thus more or less the distance between these tori and the border of the regular island which contains them. This distance is much smaller than that separating the two tunneling tori. It is therefore natural that the connecting matrix elements with neighboring chaotic states are orders of magnitude larger than the direct term and therefore that the chaotic region is assisting and playing the major role in the tunneling process.

IV. STATISTICAL MODELING

We have seen that chaos-assisted tunneling leads to quite erratic energy splittings either as an external parameter is varied or as a function of $\hbar$. In order for a detailed, comprehensive theory to reproduce the precise tunneling behavior, it must incorporate two major components and do so from within a semiclassical framework. First, the positions of the chaotic levels would have to be accurately determined on the scale of a mean level spacing. Despite the impressive recent progress toward this goal [16], it is neither clear that this will soon be possible nor that this is possible even in principle [17]. Second, the coupling matrix elements between the quasimodes and chaotic states must be calculable. This implies a detailed semiclassical understanding of the individual chaotic eigenstates (assuming the tunneling is "turned off"), which again is neither at hand nor necessarily possible; see, however, [18].

A complementary approach to tackling this question is to pursue a statistical treatment of the tunneling process. In this way a small set of essential parameters will emerge which describe properties of the distribution of tunneling splittings. One natural application would be to tunneling devices where the distribution of splittings under variation of an external parameter or averaging over the disorder is more relevant than individual values of tunneling rates. However, even without disorder or some other obvious motivation for an ensemble averaging method (consider the quartic oscillators treated ahead),

a statistical approach captures physics that would otherwise be difficult to uncover or explain. The sensitivity of chaotic motion to perturbation almost guarantees that statistical laws are in operation. The ensembles we will use, though not "derived" from some fundamental starting point, will be shown to reflect the statistical laws provided that they are properly designed to account for the relevant information, i.e., local mean square tunneling matrix elements and transport time scales.

We follow the spirit of the treatment of the spectral fluctuations of classically chaotic systems for which it is now well established that for many quantities the quantum Hamiltonian leads to the same fluctuation properties as properly chosen random matrix ensembles [19]. For strongly chaotic systems, the ensemble is taken from among Wigner's "classical ensembles" depending on the system's global symmetries; the Gaussian orthogonal ensemble (GOE) corresponds to having time reversal invariance. For mixed dynamics, such as that found in the quartic oscillators, internal structures in the chaotic region exist. They give rise to classical transport limitations which, as demonstrated in [20,10], strongly influence the quantum behavior, so that more structured ("generalized") ensembles must be introduced. For the sake of clarity, we begin by supposing that the chaotic states are correctly described by the GOE. The specific effects of classical transport limitation will be added in Sec. IV B.

A. "Classical random matrix ensembles"

If the chaotic region is supposed structureless, the following simplified matrix ensemble should capture the typical fluctuation phenomena of the chaos-assisted tunneling process. We suppose, as usual, that the quasidegeneracies occur because the system under consideration possesses some discrete symmetry. We denote Ψ^r_+ and Ψ^r_- the symmetrized and antisymmetrized tunneling regular states under study, with respective mean energies $E^r + \epsilon$ and $E^r - \epsilon$. ϵ results from the direct coupling in the two-level tunneling process. It is set to zero in what follows since we are interested in the case where chaos-assisted processes dominate. [An important problem is to determine ϵ's magnitude to know whether direct or chaos-assisted tunneling dominates. Though not discussed in this paper, both may occur in a single spectrum. This actually happens in the quartic oscillators where doublets from one particular KAM island show smooth direct tunneling behavior even though all the other doublets from the other islands have erratic, chaos-assisted behavior. The smooth behaving islands happen to lie much "closer" to each other in phase space.]

Let $\mathcal{E}^c_+$ and $\mathcal{E}^c_-$ be the quantum Hilbert spaces associated with chaotic states in the corresponding symmetry classes. The quantum Hamiltonian $\hat{H}$ projected on $\mathcal{E}^c_+$ or $\mathcal{E}^c_-$ will be modeled by a GOE. It is an ensemble of $N \times N$ symmetric matrices whose matrix elements are Gaussian random variables of uniform variance α^2, except on the diagonal where the variance is $2\alpha^2$. α must be chosen such that the mean density of chaotic states around E^r is correctly reproduced and it scales as $N^{1/2}$. In this way, N plays no other role and is of no importance. As long as N exceeds some fairly small number (typically of order 10), all the interesting statistical properties of the ensemble have converged to the appropriate $N \to \infty$ limit. Note that the $(\mathrm{GOE})^+$ and $(\mathrm{GOE})^-$ associated with $\mathcal{E}^c_+$ and $\mathcal{E}^c_-$, respectively, are independently constructed in this simplified picture. In the same spirit, it is reasonable to consider the case where the tunneling matrix elements that connect Ψ^r_+ or Ψ^r_- are uncorrelated with the GOE structure. Then the elements can be taken to behave as independent Gaussian random variables of uniform variance v^2 since only the total sum of the squared elements can have any bearing on the statistical distributions. This follows necessarily from the properties of the orthogonal transformations that diagonalize the members of the GOE. Symbolically the ensemble modeling the Hamiltonian would thus looks like

$$\hat{H}\begin{pmatrix} \Psi^r_+ \\ \mathcal{E}^c_+ \\ \Psi^r_- \\ \mathcal{E}^c_- \end{pmatrix} = \begin{pmatrix} E^r & \{v^+\} & 0 & 0 \\ \{v^+\} & (\mathrm{GOE})^+ & 0 & 0 \\ 0 & 0 & E^r & \{v^-\} \\ 0 & 0 & \{v^-\} & (\mathrm{GOE})^- \end{pmatrix} \times \begin{pmatrix} \Psi^r_+ \\ \mathcal{E}^c_+ \\ \Psi^r_- \\ \mathcal{E}^c_- \end{pmatrix}. \tag{22}$$

The + and − superscripts emphasize the independent nature of the matrix elements in the different symmetry classes.

Perturbative nature

As previously stated, a semiclassical theory to compute the variance of the tunneling matrix element v^2 is still lacking; note that this is likely to be a much simpler problem than trying to calculate each individual matrix element. However, the matrix ensemble, Eq. (22), can be studied now as a pure random matrix problem, providing us with a definite prediction for the splitting distribution. It has qualitative behaviors which can be understood on a general footing. A simplifying feature, for instance, is due to the fact that the matrix elements connecting the regular states to the chaotic space are due to classically forbidden processes. For tori deep within the KAM region the ratio $v/D_\pm$ [where $D_\pm$ is the mean energy spacing for the $(\pm)$ chaotic states] is always much smaller than one. Leading order degenerate perturbation theory will give an excellent approximation to exact results.

For a given chaotic spectrum $(E^+_1, \ldots, E^+_N, E^-_1, \ldots, E^-_N)$ and tunneling matrix elements $(v^+_1, \ldots, v^+_N, v^-_1, \ldots, v^-_N)$, the displacements δ^+ and δ^- of the regular states energies are given by

$$\delta^\pm/D = \frac{1}{2}\sum_{n=1}^{N} r^\pm_n - \mathrm{sgn}(r^\pm_n)\sqrt{(r^\pm_n)^2 + 4(v^\pm_n)^2/D^2}\,, \tag{23}$$

in which $r^\pm_n$ is defined as $r^\pm_n = (E^\pm_n - E^r)/D$. The tun-

neling splitting δ is then the magnitude $\delta = |\delta^+ - \delta^-|$. As stated below Eq. (6.1) of [10] (see also [21]), the above approximation can be understood as coming from a separate contribution of each of the different chaotic states. One then uses the exact 2×2 diagonalization results term by term and finally sums all the individual contributions. If all levels are distant, the right-hand side of Eq. (23) is equal to the Rayleigh-Schrödinger perturbation result excluding higher order corrections. It moreover matches smoothly the degenerate perturbation result when one chaotic level approaches E^r closely. The rarity of three or more levels being found nearly degenerate leads also to higher order corrections in the splitting distribution and can be ignored.

Equation (23) implies the distinctive property that an order of magnitude difference exists between a "typical splitting" and, say, the root mean square deviation of the distribution. The reason for this is that most often no chaotic level approaches E^r more closely than the typical size v of the tunneling matrix element. In such a situation, Eq. (23) can be replaced by the usual nondegenerate perturbative result

$$\delta^{\pm}/D = -2\sum_{n=1}^{N} \frac{1}{r_n^{\pm}} \frac{(v_n^{\pm})^2}{D^2} , \tag{24}$$

which leads to a splitting of order $\delta/D \sim v^2/D^2$. In rare circumstances with probability of order v/D, a chaotic level $E_n^{\pm}$ does manage to be nearly degenerate with E^r. The associated contribution to Eq. (23) is then of order v/D (measured in units of the mean spacing) and dominates the splitting. Such events give the leading contribution to all moments of the distribution of order m equal or greater than 2 because, roughly speaking, their contribution is of order $(v/D)^m(v/D)$ whereas the rest of the splittings contribute $(v/D)^{2m}$.

Consider the leading order calculation of the splitting variance $\overline{\delta^2}$ (the bar indicates ensemble averaging). It can be written as

$$\overline{\delta^2} = \overline{(\delta^+)^2} + \overline{(\delta^-)^2} + \overline{2(\delta^+)(\delta^-)} = 2\overline{(\delta^{+(-)})^2} . \tag{25}$$

The last form relies on the uncorrelated relationship between the + and − GOE. Working, for instance, with δ^+, one has, using Eq. (23),

$$\begin{aligned}\left(\frac{\delta^+}{D}\right)^2 &= \frac{1}{4}\sum_{n\,n'}\left[r_n^+ - \mathrm{sgn}(r_n^+)\sqrt{(r_n^+)^2 + 4(v_n^+)^2/D^2}\right]\left[r_{n'}^+ - \mathrm{sgn}(r_{n'}^+)\sqrt{(r_{n'}^+)^2 + 4(v_{n'}^+)^2/D^2}\right] \\ &= \frac{1}{4}\sum_{n}\left[2(r_n^+)^2 + 4(v_n^+)^2/D^2 - 2|r_n|\sqrt{(r_n^+)^2 + 4(v_n^+)^2/D^2}\right] \\ &\quad + \frac{1}{4}\sum_{n\neq n'}\left[r_n^+ - \mathrm{sgn}(r_n^+)\sqrt{(r_n^+)^2 + 4(v_n^+)^2/D^2}\right]\left[r_{n'}^+ - \mathrm{sgn}(r_{n'}^+)\sqrt{(r_{n'}^+)^2 + 4(v_{n'}^+)^2/D^2}\right] .\end{aligned}$$

The ensemble average is performed [22] by replacing the v_n by independent Gaussian variables of variance v^2 and by making the substitutions

$$\sum_n \longrightarrow \int dr, \quad \sum_{n\neq n'} \longrightarrow \int dr\, dr' R_2(r-r') ,$$

where r (r') is the energy measured in mean spacing unit and $R_2(r-r')$ the GOE two-point correlation function [23]. Therefore the ensemble average $\overline{(\delta^+)^2}$ is the sum of two contributions I_1 and I_2,

$$I_1 = \frac{1}{4}\int dr \int dw \frac{e^- w^2/2}{\sqrt{2\pi}}\left(2r^2 + 4w^2v^2/D^2 - 2|r|\sqrt{r^2 + 4w^2v^2/D^2}\right) = \frac{32(v/D)^3}{3\sqrt{2\pi}} \tag{26}$$

and

$$I_2 = \frac{1}{4}\int dr\, dr' R_2(r-r') \int dw\, dw' \frac{e^-(w^2+w'^2)/2}{2\pi} \times \left[r - \mathrm{sgn}(r)\sqrt{r^2 + 4w^2v^2/D^2}\right] \times \left[r' - \mathrm{sgn}(r')\sqrt{r'^2 + 4w'^2v^2/D^2}\right] , \tag{27}$$

the latter being of order $(v/D)^4\log^2(v/D)$. The variance of the splitting to leading order is

$$\frac{\overline{\delta^2}}{D^2} = \frac{64(v/D)^3}{3\sqrt{2\pi}} . \tag{28}$$

As just mentioned, it is easily seen that the contribution arising from spectra for which no chaotic state is closer to E^r than some arbitrary, small (but fixed) distance μ (i.e., a proportion $1-\mu$ of the configurations) is only of order $(v/D)^4$.

So two kinds of tunneling splittings can be distinguished in the random matrix model, just as is true of the quartic oscillators spectrum: (i) small splittings of order v^2/D^2, which correspond to nearly all events, and

(ii) relatively large splittings (still quite small though) of order v/D associated with chaotic state crossings. This occurs extremely rarely, but gives rise to the dominant contribution to the moments of the distribution of order 2 or greater. Note that because the quasimode and chaotic state may mix strongly here, it can on rare occasions even be ambiguous as to which two levels form the tunneling pair from the three of them. These two kinds of splittings may be of a rather different character. In particular we shall see that they react quite differently to classical transport limitations.

B. Classical transport effects: Generalized ensembles

One source of the richness of mixed system dynamics is that usually even the chaotic regions possess some inner structure (significant time scales beyond a mixing time) [24,25]. They play a noticeable role in various physical situations and their effects have, for instance, been extensively investigated in the study of chemical reaction rates [26,27]. A large variety of mechanisms limiting the transport may exist, among which one of the simplest occurs when the transport is dominated by a limited number of well separated partial barriers; see [10]. In such a situation, the chaotic part of the phase space can be divided into a certain number of subregions $\mathcal{R}_1, \mathcal{R}_2, \ldots, \mathcal{R}_n$, in which a trajectory seems to be trapped for a while before it eventually travels to a neighboring subregion. The rate of communication between two regions $\mathcal{R}_i$ and $\mathcal{R}_j$ can be characterized by the classical flux Φ_{ij} connecting them, i.e., the phase space volume per unit time exchanged from one region to the other. It is this kind of transport that is found for the quartic oscillators system in the mixed regime. Figure 8 illustrates the subregions of the quartic oscillators as viewed from a surface of section. As demonstrated in [10], the chaotic levels' spectral fluctuations, as well as some statistical properties of the wave functions, reflect the transport limitations. These properties are correctly described using a modeling of the chaotic dynamics in terms of "generalized ensembles," the parameters of which are entirely fixed by the classical motion. For *each* symmetry class, one may summarize the construction of the generalized ensemble as follows (see Sec. 5 of [10] for more details): (i) to each region $\mathcal{R}_i$, associate a Hilbert subspace $\mathcal{E}_i^c$ inside which the projection of the Hamiltonian matrix is taken as a Gaussian ensemble $(\mathrm{GOE})_i$, such that the corresponding mean spacing is proportional to the phase space volume of $\mathcal{R}_i$; (ii) connect the blocks i and j by matrix elements taken as independent Gaussian variables of variance α_{ij}^2 such that the "transition parameter"

$$\Lambda_{ij} \equiv \frac{\alpha_{ij}^2}{D^2} \tag{29}$$

is fixed (D is the total mean spacing). The transition parameter determines the properties of the ensemble as stressed in [22]. It naturally emerges in perturbation theory treatments of weakly broken symmetries, but is more general. It arises here because the small classical flux can be thought of as breaking the dynamical symmetry which isolates the subregions $\mathcal{R}_i$ and their respective Hilbert subspaces $\mathcal{E}_i^c$. Λ_{ij} is related to the classical flux Φ_{ij} by [10,20]

$$\Lambda_{ij} = \frac{1}{4\pi^2} \frac{g\Phi_{ij}}{(2\pi\hbar)^{d-1} f_i f_j} . \tag{30}$$

Here g is the proportion of states in the considered symmetry class, d the number of degrees of freedom, and f_i the relative phase space volume of region $\mathcal{R}_i$. Symbolically, we shall refer to such an ensemble using (for $n = 2$) the notation

$$\hat{H} = \begin{pmatrix} (\mathrm{GOE})_1 & \Lambda_{12} \\ \Lambda_{12} & (\mathrm{GOE})_2 \end{pmatrix} . \tag{31}$$

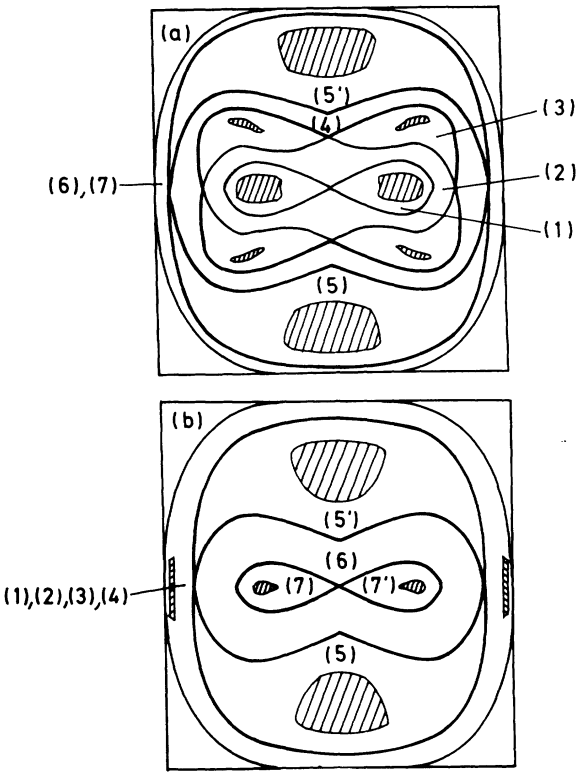

FIG. 8. Chaotic subregions imperfectly isolated by partial transport barriers for the case $(\lambda, b) = (-0.35, \pi/4)$: (a) $q_1 = 0$ Poincaré section; (b) $q_2 = 0$ Poincaré section. The regular islands are also outlined. Also given in Ref. [10].

Treatment of induced correlations

We are considering a problem in which two KAM islands are distinct, but transform into each other by a discrete symmetry operation. Suppose there existed one or more completely closed (perfect) transport barriers in the chaotic region of phase space that prevented flow from near one island to the neighborhood of its partner. The chaotic subregions around each KAM island would be

just as isolated, distinct, and symmetry related as the islands themselves. Under these circumstances, they would themselves give rise to quasidegeneracies in the spectrum just as quantized tori pairs do. In addition, the tunneling matrix elements would be identical by the same discrete symmetry consideration. The ensemble would have the form of Eq. (22) except that $\{v^-\} = \{v^+\}$ and $(\mathrm{GOE})^+ = (\mathrm{GOE})^-$, matrix element by matrix element. Under these circumstances, Eq. (23) would give a zero splitting. However, our interest is in imperfect transport barriers. In this case the tunneling splittings are not zero, only reduced. This occurs by the introduction of correlations in the different symmetry classes of the chaotic spectrum and in the tunneling matrix elements as well.

The simplest classical configuration of interest incorporating some partial barriers is the one schematized in Fig. 9. The two tunneling tori belong to two regions $\mathcal{R}_1$ and $\mathcal{R}_1{}'$ symmetric with respect from each other. Transport between $\mathcal{R}_1$ and $\mathcal{R}_1{}'$ takes place through a third, slightly connected (symmetric) region $\mathcal{R}_2$. As shown in Appendix B, the associated generalized ensemble has, for the different symmetry classes, the form

$$\hat{H}^{\pm} = \begin{pmatrix} E^r & \{v\} & 0 \\ \{v\} & (\mathrm{GOE})_1 & \Lambda_{12} \\ 0 & \Lambda_{12} & (\mathrm{GOE})_2^{\pm} \end{pmatrix} . \qquad (32)$$

Again $(\mathrm{GOE})_2^{\pm}$ indicates that the + and − $(\mathrm{GOE})_2$'s are uncorrelated. In the limit that $\Lambda_{12} \to 0$, the splittings are zero (perfect correlations). In the opposite limit $\Lambda_{12} \to \infty$, the ensemble of Eq. (22) is recovered (absence of correlations).

As far as the chaotic states are concerned, the variations of Λ_{12} not only modify the correlations between symmetry classes, but also in general the various spectral statistics that one may define inside each symmetry class. For the tunneling states, however, the value of Λ_{12} has little influence on the distribution of displacements δ^+ and δ^-. To see this, let us consider the two extreme cases $\Lambda_{12} = 0$ and $\Lambda_{12} \to \infty$. For simplicity assume that $\mathcal{R}_1$ and $\mathcal{R}_2$ have the same phase space volume, i.e., that the mean spacing D_1 and D_2 associated, respectively, with $(\mathrm{GOE})_1$ and $(\mathrm{GOE})_2$ are the same ($D_1 = D_2 = 2D_{\mathrm{tot}}$, where D_{tot} is the total mean spacing). To diagonalize the chaotic part of the Hamiltonian for $\Lambda_{12} \to \infty$ essentially amounts, as compared to $\Lambda_{12} = 0$, to transferring half the variance of the tunneling matrix elements from chaotic states associated to $\mathcal{R}_1$ to others associated to $\mathcal{R}_2$.

Thus, in both cases, the tunneling state is connected to a full GOE. Moreover, if one denotes by v_{eff}^2 the effective (i.e., after diagonalization) variance of tunneling matrix elements and by D_{eff} the mean spacing of chaotic states effectively playing some role in the tunneling process, one has

$$v_{\mathrm{eff}}^2(\Lambda_{12} \to \infty) = \frac{v^2}{2}, \quad D_{\mathrm{eff}}(\Lambda_{12} = 0) = D_1 = 2D_{\mathrm{tot}} .$$

Therefore, going through the whole range of variation of Λ_{12} leads only to a factor $\sqrt{2}$ change between the tunneling parameters $v_{\mathrm{eff}}^2/D_{\mathrm{eff}}(\Lambda_{12} = 0)$ and $v_{\mathrm{eff}}^2/D_{\mathrm{eff}}(\Lambda_{12} \to \infty)$. This factor is extremely small as compared to the range of variation spanned by the splitting distribution (usually a few orders of magnitude). In addition, one is interested in the distribution of $\delta^{\pm}/D_{\mathrm{tot}}$ since D_{eff} can be given a meaning only for the extreme cases $\Lambda_{12} = 0$ and $\Lambda_{12} \to \infty$, but not in the whole range of variation of Λ_{12}. In $\log_{10}$ binning, this just consists in shifting the distribution of $\delta^{\pm}/D_{\mathrm{eff}}$ a distance $\log_{10}(2)$ to the right for $\Lambda_{12} = 0$, which goes the other way round as what is due to the change in the effective tunneling parameter. The resulting effect of these two small mechanisms which work in opposite directions is to leave the distribution of $\delta^{\pm}/D_{\mathrm{tot}}$ essentially unchanged when going from $\Lambda_{12} = 0$ to $\Lambda_{12} \to \infty$. Indeed, when comparing a Monte Carlo calculation of these distributions on Fig. 10, they appear almost indistinguishable. It has been checked moreover that this remains true for intermediate values of Λ_{12}.

Returning to the distribution for δ, the correlations between δ^+ and δ^- become important. It is clear that for $\Lambda_{12} = 0$, δ^+ is perfectly correlated to δ^- and for $\Lambda_{12} \to \infty$ they are uncorrelated. For $\Lambda_{12} > 0$ but small, we recall the most significant feature of ensembles modeling weakly broken symmetries [22] — the transition in fluc-

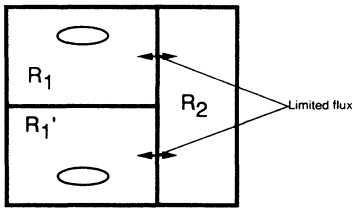

FIG. 9. Schematic illustration of the phase space structure linked with the ensemble of Eq. (32). Regions R_1 and R_1' are identical by symmetry and are dynamically connected by their fluxes leaking into region R_2. The ellipses represent the KAM regions.

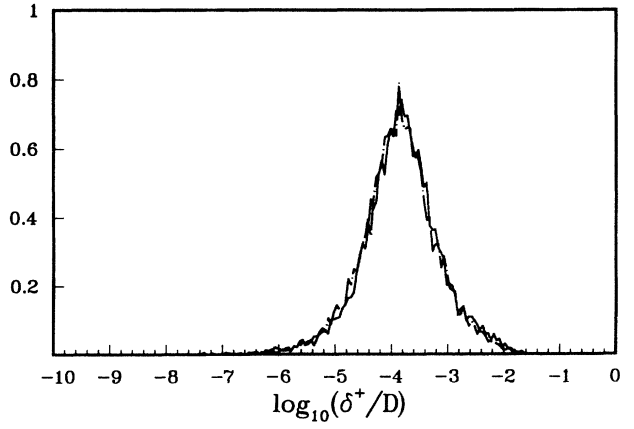

FIG. 10. The distribution of δ^+'s motions deriving from the ensemble of Eq. (32) (with $v/D = 0.01$) for $\Lambda_{12} \to \infty$ (solid line) and $\Lambda_{12} = 0$ (interrupted line). The two curves are hardly distinguishable, in contrast with the effect on δ itself. See Fig. 11.

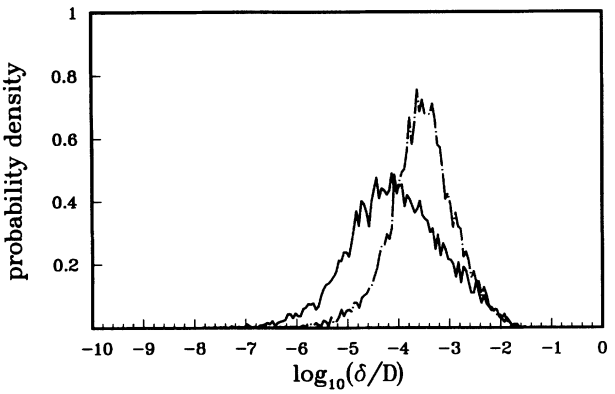

FIG. 11. The distribution of splittings δ for the ensemble of Eq. (32) with $v/D = 0.01$. Partial transport barriers broaden the distribution by having little effect on the large splittings and reducing the small splittings due to induced long range correlations in the chaotic spectra. Pictured are the cases $\Lambda \to \infty$, which correspond to an absence of partial barrier (dash-dotted line, sharper peak) and $\Lambda = 0.1$ (solid line, broader curve).

tuation properties with increasing Λ sweeps from short range out to long range. Here, for example, the correlations between the + and − spectra disappear at short range first while the long range structure of the spectrum is still highly correlated. The weak splittings dependent on the multilevel mechanism, and thus on many distant levels, will be considerably affected and reduced by correlations induced by transport. On the other hand, for the large splittings due to a chaotic level closer to E^r than v/D (which being due to a classically forbidden process is smaller than $\Lambda^{1/2}$, i.e., $v/D \ll \Lambda^{1/2} \ll 1$), little or no effect of the transport barrier is visible. Though the mean tunneling may overall be smaller, the most significant effect renders the small splittings smaller and increases the width of the splitting distribution. This is illustrated in Fig. 11. Therefore the splitting distribution is not universal, depending on both the chaotic transport and the tunneling matrix element variance.

C. The return of the quartic oscillators

In the preceding subsection, we have used the prescription devised in [10] to construct random matrix ensembles accounting for the effects of partial transport barriers that model the splitting distribution. Note the model is entirely specified by the classical dynamics, without free parameters. The random matrix model predicts that the partial barriers have little effect on the distributions of the displacements δ^+ and δ^-, at least on the scale they span. On the other hand, the fact that classical trajectories are prevented to flow freely from the neighborhood of one torus to the one of its symmetric partner induces correlations between δ^+ and δ^-, yielding a noticeable modification of the splitting distribution ($\delta = |\delta^+ - \delta^-|$). The qualitative way in which this distribution is modified is interpretable from the general behavior of transition ensembles like the one of Eq. (31).

The relevance of the generalized ensembles to chaos-assisted tunneling can be stringently tested with the coupled quartic oscillators' spectrum. To uniquely construct the ensembles, we need the structure of the chaotic region in phase space and the fluxes Φ_{ij}. We also need the mean square tunneling matrix element for which there currently is no semiclassical theory. v^2 could be taken as a free parameter with interesting results, but a more exacting procedure is available by extracting it directly from the spectrum. This is discussed more fully below. As a practical matter note that observing a distribution which spans many orders of magnitude is made easier by using the logarithm of the splitting ($\log_{10}\delta_{n_1,n_2}$), which is done from here on; n_1,n_2 refers to the number of quanta on each cycle J_1 and J_2 of the quantizing torus.

Consider a single doublet labeled by (n_1, n_2). Its splitting can be calculated for a large number of values over a narrow range of λ. The point of keeping λ's range narrow is to ensure that the structures in the classical dynamics change very little. The range $\lambda \in [-0.36, -0.32]$ is used in the following so that use of the fluxes and structures for $\lambda = -0.35$ as detailed in [10] are representative of the entire range. For $\hbar$ small (E large), the doublet will nevertheless cross many levels; the range is thus small on the classical scale but broad on the quantum scale. In our calculation, we determined the lowest 4100 levels for 201 values of λ to sufficient accuracy, $\sim 10^{-6}D$. It is found that a single doublet deep from within the KAM island crosses, on average, around 20 chaotic levels in this interval. A distribution of splittings can thus be constructed from a single pair. Going a bit further to improve the statistical significance, 17 consecutive pairs near the top of the spectrum were identified with $n_1 = 0$ and their splittings were combined to form one distribution based on ~ 3500 values. A second set of 6 consecutive doublets with $n_1 = 1$ were also put together. The distinction between the two groups is that the local collection of tori associated with the $n_1 = 1$ group is 3 times further from the center of the KAM island than the $n_1 = 0$ tori. The tori with $n_1 = 2$ or 3 proved to be too time consuming to work with since they were too close to or outside the KAM-chaos interface for the size of $\hbar$ (energy).

The appropriate generalized ensemble incorporates the classical phase space structure of Fig. 8 relevant to the tunneling process, which is schematized in Fig. 12. The

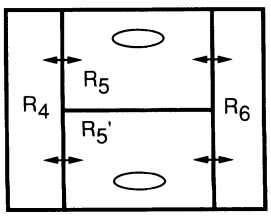

FIG. 12. Schematic of the most important phase space and transport structure of the quartic oscillators surrounding islands 1 (see Fig. 8). The islands are represented by the ellipses. Trajectories must pass through either region R_4 or R_6 to travel from the neighborhood of one KAM region to the other.

two groups of tunneling tori T_0 ($n_1 = 0$) and T_1 ($n_1 = 1$) are in two symmetric regions $\mathcal{R}_5$ and $\mathcal{R}_5'$. To travel from $\mathcal{R}_5$ to $\mathcal{R}_5'$, a classical trajectory must first jump into either $\mathcal{R}_4$ or $\mathcal{R}_6$ before continuing to $\mathcal{R}_5'$. There also exist further outside regions $\mathcal{R}_1$, $\mathcal{R}_2$, $\mathcal{R}_3$, and $\mathcal{R}_7$, which are only slightly connected at the considered energy and do not play a noticeable role. In the same way as in Sec. IV B, it can be seen that the ensemble for the symmetry class + or − is (see Appendix B)

$$\hat{H}^{\pm}\begin{pmatrix}\Psi_{\pm}^{r}\\ \mathcal{E}_5^c\\ \mathcal{E}_4^c\\ \mathcal{E}_6^c\end{pmatrix} = \begin{pmatrix} E^r & \{v\} & 0 & 0\\ \{v\} & (\mathrm{GOE})_5 & \Lambda_{45}^{\pm} & \Lambda_{56}^{\pm}\\ 0 & \Lambda_{45}^{\pm} & (\mathrm{GOE})_4^{\pm} & 0\\ 0 & \Lambda_{56}^{\pm} & 0 & (\mathrm{GOE})_6^{\pm}\end{pmatrix} \times \begin{pmatrix}\Psi_{\pm}^{r}\\ \mathcal{E}_5^c\\ \mathcal{E}_4^c\\ \mathcal{E}_6^c\end{pmatrix}. \tag{33}$$

The superscript ± specifies blocks which are independent in the two symmetry classes. Its absence means that the block is the same. In Eq. (33), $(\mathrm{GOE})_4$, $(\mathrm{GOE})_5$, and $(\mathrm{GOE})_6$ are such that their mean spacings are proportional to the the relative phase space volumes f_i ($i = 4, 5, 6$) of the associated regions and Λ_{45} and Λ_{56} are related to the fluxes Φ_{45} and Φ_{56} through Eq. (30). The necessary classical quantities are gathered in Table II.

We turn to determining the variance v^2 of the tunneling matrix elements. It has already been seen in Fig. 7 that the crossings of regular and chaotic levels behave as though they are isolated. A single realization from $\{v\}$ comes with each such crossing in the spectra. Following the procedure mentioned in the last paragraph of Sec. III, 310 values of $\{v\}$ were found for the T_0 doublets and 110 for the T_1 doublets. The largest values obtained in this way are the most accurate since, not surprisingly, their plateaux are typically the broadest. Those realizations a few orders of magnitude weaker are more uncertain. A method to calculate v^2 is therefore more reliable if it is based on the large members of $\{v\}$. Furthermore, recall that diagonalizing the chaotic part of the Hamiltonian transfers some tunneling matrix elements from the block connecting $\mathcal{E}_5^c$ to other ones. The spectrum itself reflects the redistributed $\{v\}$ and not the one of Eq. (33). Because at the considered energy fluxes are rather small, this will only slightly lower the variance of the tunneling matrix elements in the former block. It will create many very small elements of $\{v\}$ where previously the ensemble had zeros. It is best to avoid the small realizations altogether. Roughly speaking, only the fraction f_5 of the larger tunneling matrix element values corresponds to a crossing with a chaotic state living in $\mathcal{R}_5$. To be more precise, the upper tail of the tunneling matrix element distribution should correspond to f_5 times the tail of a Gaussian distribution of width v, i.e., in a logarithmic binning

$$\rho(x) = f_5 \frac{\mathrm{e}^{-x^2/2v^2}}{\sqrt{2\pi}} \frac{x\ln(10)}{v}. \tag{34}$$

In practice, having only a few hundred crossings, it is necessary to somewhat smooth the fluctuations in the tail of the distribution. For a wide range of the smoothing width, the value of v obtained from a least-squares deviation from the tail of the matrix element distribution and Eq. (34) remains extremely stable and is independent of the smoothing. It leads to a value of v/D approximately 1.1×10^{-2} for both groups T_0 and T_1. The reason why the two values are nearly the same is essentially due to the competing effects of T_1 being closer to the boundary

TABLE II. Relative volume f_i of chaotic phase space of the regions relevant to the tunneling process, together with their connecting flux (taken from [10]). The fluxes are calculated for $E = 1$ and scale as $E^{3/4}$. From this table and Eq. (30) (note $g = 1/4$) all the parameters of the ensemble of Eq. (33) are specified, except for the variance v^2 of the tunneling matrix elements.

Region	Relative volume f_i	Total flux	
4	0.13		
		$4 \leftrightarrow 5$	0.21
5	0.36		
		$5 \leftrightarrow 6$	0.28
6	0.21		

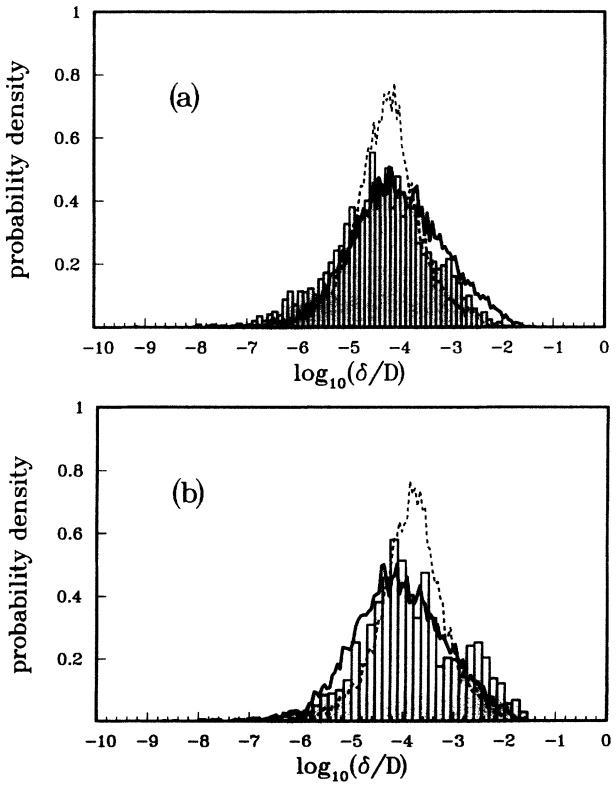

FIG. 13. Comparison of the quartic oscillator's tunneling splitting distribution to the random matrix ensemble predictions. The histogram displays the results for the quartic oscillators (a) of the T_0 group of tori and (b) of the T_1 group of tori. The solid curve is the prediction of the generalized random matrix ensemble incorporating the transport information (see text). The peaked dashed curve is a best fit using a single GOE for the chaotic region (no transport barriers).

of the island, but also at slightly smaller $\hbar$ (higher energy) on average. It is reasonable that the former effect compensates the first because the tunneling shrinks with $\hbar$, but T_1 doublets cross the chaotic levels with a smaller slope.

Inserting the obtained values into the ensemble of Eq. (33) gives the comparison between the $(\log_{10}\delta_{n_1,n_2})$ distribution and the Monte Carlo prediction displayed in Fig. 13. Also shown is a comparison using a best value of v for which the classical phase space structure has not been implemented. In the former case one obtains a nice correspondence between the predicted and the calculated curve whereas in the latter, a clear discrepancy is observed despite the use of a free parameter. This is strong evidence of the relevance of the generalized ensemble introduced to model the splitting distribution. It is also another signature of the importance of the classical dynamics inside the chaotic zone as concerns the tunneling process [11].

V. CONCLUSIONS

We have shown that the nature of the underlying classical dynamics deeply affects how tunneling takes place. In principle, the vast range in complexity of dynamics implies a wealth of tunneling phenomena. Considering that in multidimensions even the simplest case, i.e., integrable motion, is not a fully resolved problem, there remains a great deal to uncover.

From a dynamical point of view, most systems at some fixed energy are mixed in that they contain both significant regions of regular and chaotic motion. The corresponding quantum systems have classes of both regular (quantizing tori) and chaotic eigenstates. Systems with discrete symmetries may give rise to multiple copies of the tori and then there exist states (quasimodes) which are degenerate to any power of $\hbar$. Tunneling lifts the degeneracies either directly or through chaos assisted processes. The roughest statement of the difference between the two mechanisms is that chaos assistance involves otherwise extraneous chaotic levels which act as intermediaries for the tunneling process. This is embodied in the simplest way by the three-level model described in Sec. II B. The system of coupled quartic oscillators were especially well suited to demonstrating these points.

Very little is understood about the magnitudes of these mechanisms leaving open many interesting questions. One of the more important is being able to predict, under a given set of circumstances, whether one process (chaos-assisted or direct) should dominate the other and if so, which one. No attempt was made here to derive such a theory, which is left for future study. Instead we focused on giving evidence for chaos-assisted tunneling and describing its major features. Since this tunneling proceeds through chaotic level intermediaries, one component of a semiclassical theory must be the description of chaotic eigenproperties. However, there are fundamental reasons to suspect that this may be impossible. Whether it is true or not, the necessary theory does not currently exist. On the other hand, the statistical eigenproperties have been discussed at length in [10,20]. Properties of level fluctuations, wave function localization, etc. have all been linked to various features of chaotic phase space and transport structures. Those ideas are extended here to develop an interpretation of the splitting distribution involving generalized ensembles within random matrix theory; both three-level and multilevel mechanisms appear in the ensemble. With the transition parameter–classical flux relation Eq. (30), the classical transport can be transformed into constraints on the random matrix ensemble modeling the quantum system. (More complicated kinds of transport problems than those which arise in the quartic oscillators' spectra discussed here may not be so easily transcribed into appropriate ensembles. Other, new tunneling effects not mentioned in this work may be found in conjunction with those cases.) The only problem (or rather parameter) remaining is to determine the mean square tunneling matrix element v^2 (or equivalently v^2/D^2) connecting regular and chaotic states. v^2 can be extracted from a spectrum though and the quartic oscillators' spectrum clearly confirms that the splitting distribution is given by the ensemble theory if and only if transport properties and v^2 information is properly included. A theory of v^2 is part of discovering whether chaos-assisted tunneling is the most important process. While this description is far from existing, tantalizing glimpses have been found in the spectra in which $\hbar$, the resonance structure of the KAM region, and the position of the particular tori (that v^2 is connecting to the nearby chaotic zone) all play a role.

The realization and detection of chaos-assisted tunneling ought to be possible in a number of ways. Molecular systems have anharmonic potentials governing their chemical bonds. As long as a sufficient density of states with sufficient anharmonicity can be observed without breaking down the Born-Oppenheimer approximation, chaos-assisted tunneling would take place between symmetric local modes. There are also a number of possibilities with microwave cavities and low temperature mesoscopic tunneling devices. The sensitivity of the tunneling to the influence of the variation of an external parameter should provide a clearcut signal of its existence in a particular system.

ACKNOWLEDGMENTS

One of us (S.T.) would like to acknowledge support from the National Science Foundation Grant No. PHY-9305582 with additional support from Grant No. DMR-8916052. The Division de Physique Théorique is "Unité de Recherche des Universités Paris 11 et Paris 6 Associée au CNRS."

APPENDIX A: LANGER CONNECTION FORMULA

We recall the connection formula derived by Langer in [12]. Consider the one-dimensional Schrödinger equation

$$\frac{-\hbar^2}{2m}\Delta\Psi + V(q)\Psi = E\Psi\,, \tag{A1}$$

with a potential such that

$$V(q) \geq E \quad \text{for } q < q_1, \quad V(q) \leq E \quad \text{for } q > q_1.$$

Far from the turning point q_1, the general form of the semiclassical approximation to the solution of Eq. (A1) is (except for a multiplicative constant)

$$\Psi(q) = \begin{cases} \frac{2}{\sqrt{p}} \cos(S/\hbar - \pi/4 + \eta) & \text{for } q < q_1 \\ \frac{1}{\sqrt{p}} (2 \sin\eta \, e^{|S|/\hbar} + \cos\eta \, e^{-|S|/\hbar}) & \text{for } q > q_1, \end{cases}$$

where p is given by Eq. (4) and S by

$$S(q) = \int_{q_1}^{q} |p| \, dq \, . \tag{A2}$$

Therefore η, which is the difference from $\pi/2$ of the dephasing between the incoming and the outgoing wave on the left of the turning point, is controlling the amplitudes of the exponentially increasing and decreasing terms on the right of q_1. In Sec. II, the above connection formula is used in its simplest form to construct two wave functions; i.e., either $\eta = 0$ (only the decreasing exponential) or $\eta = \pi/2$ (only the increasing one).

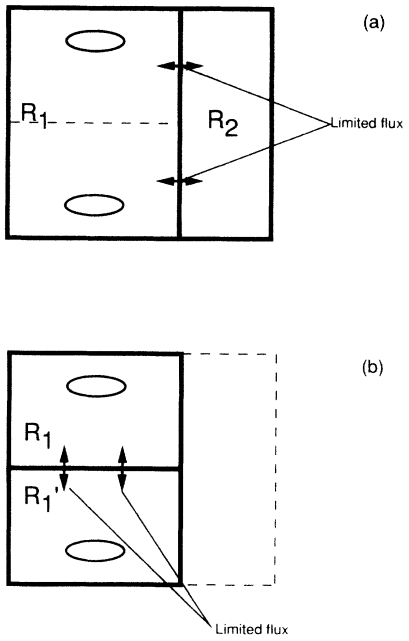

FIG. 14. Schematic of the phase space structures corresponding to (a) the ensemble of Eq. (B1) and (b) the ensemble of Eq. (B3). The dotted lines correspond to changes in the barriers which were present in the classical configuration of Fig. 9.

APPENDIX B: CONSTRUCTION OF THE ENSEMBLES

In this appendix, we show that the ensemble Eq. (32) is actually associated with the classical transport configuration depicted in Fig. 9. This is done using essentially the same kind of procedures that were used in [10] to construct ensembles such as Eq. (31). Although this paper is as self-contained as possible, a reading of Sec. 5 of [10] simplifies the understanding of what follows. Some notions, such as the introduction of a basis "relevant" to the classical structure, are best gleaned there.

As stressed in the text, the splitting distribution associated with the ensemble Eq. (32) differs from the one without transport Eq. (22) because of two distinct features. First the distribution of the displacements δ^+ and δ^- of the regular energy levels are modified. Second they become positively correlated, so that the splitting $\delta = |\delta^+ - \delta^-|$ can be significantly smaller than $|\delta^+|$ and $|\delta^-|$. Before turning to the construction of the ensemble Eq. (32), let us consider two separate transport configurations in which each feature is isolated.

1. Pure cases

The first of the above effects already exists if, starting from the classical configuration of Fig. 9 one suppresses the barrier separating $\mathcal{R}_1$ and $\mathcal{R}_1'$, leading to the configuration shown in Fig. 14(a). On the other hand, in that case all the classical chaotic regions are symmetric under the symmetry P interchanging the two tunneling tori, so that the δ^+ and δ^- are decorrelated. The remaining partial barrier can therefore be treated in exactly the same way as in [10]. (This is not because all chaotic regions were symmetric in [10], but rather due to a lack of motivation to study the correlations between symmetry classes. We simply identified regions symmetric to each other.) Namely, this means that, for each symmetry class, the $(\text{GOE})^{\pm}$ of the ensemble Eq. (22) has to be replaced by the more structured ensemble Eq. (31). Since tunneling states remain connected only with chaotic states living in region 1 one obtains

$$\hat{H}^{\pm} = \begin{pmatrix} E^r & \{v^{\pm}\} & 0 \\ \{v^{\pm}\} & (\text{GOE})_1^{\pm} & \Lambda_{12}^{\pm} \\ 0 & \Lambda_{12}^{\pm} & (\text{GOE})_2^{\pm} \end{pmatrix}, \tag{B1}$$

which is already the ensemble Eq. (32), except that the correlations between the two symmetry classes are absent.

Correlations between symmetry classes are indeed intimately related to the difficulty a trajectory has to go from one region to its symmetric. This exists if, as in Fig. 14(b), the region $\mathcal{R}_2$ of Fig. 9 does not exist, but small transport is allowed across the common boundary of $\mathcal{R}_1$ and $\mathcal{R}_1'$.

To then work out the induced correlations, let us consider a basis of the chaotic space $(|1,\alpha\rangle, |1',\beta\rangle)$ $(\alpha, \beta = 1, 2, \ldots)$, which is relevant to the classical structure, i.e., such that the $|1,\alpha\rangle$ "semiclassically" belong to $\mathcal{R}_1$ and $|1',\beta\rangle$ "semiclassically" belongs to $\mathcal{R}_1'$. To take into account the discrete symmetry P relating the two tunneling tori, we shall moreover require that $|1',\alpha\rangle = P|1,\alpha\rangle$ $(\alpha = 1, 2, \ldots)$. It is in such a "relevant basis" (see Sec. 5 of [10]) that (the chaotic part of) the Hamiltonian can be modeled by a generalized ensemble such as Eq. (31).

Therefore, noting Ψ_1^r and $\Psi_1^{r\prime}$ the tunneling states and $\mathcal{E}_1^c$ and $\mathcal{E}_1^{c\prime}$ the Hilbert subspaces associated with $\mathcal{R}_1$ and $\mathcal{R}_1{}'$, the Hamiltonian matrix expressed in the above basis can be written as

$$\hat{H}\begin{pmatrix}\Psi_1^r\\ \mathcal{E}_1^c\\ \Psi_1^{r\prime}\\ \mathcal{E}_1^{c\prime}\end{pmatrix}=\begin{pmatrix}E^r & \{v_1\} & 0 & 0\\ \{v_1\} & \hat{H}_{11}^c & 0 & \hat{H}_{1'1}^c\\ 0 & 0 & E^r & \{v_1'\}\\ 0 & \hat{H}_{11'}^c & \{v_1'\} & \hat{H}_{1'1'}^c\end{pmatrix}\begin{pmatrix}\Psi_1^r\\ \mathcal{E}_1^c\\ \Psi_1^{r\prime}\\ \mathcal{E}_1^{c\prime}\end{pmatrix}. \tag{B2}$$

Using now that $\hat{H}$ commutes with P readily gives that

$$\hat{H}_{11}^c=\hat{H}_{1'1'}^c;\quad \{v_1\}=\{v_1{}'\}\ (=\{v\}),$$

and that $\hat{H}_{1'1}^c\ (=\hat{H}_{11'}^c)$ is a symmetric matrix. Thus $\hat{H}_{11}^c=\hat{H}_{1'1'}^c$ can be modeled using a Gaussian ensemble $(\mathrm{GOE})_D$, which reproduces correctly the mean density of states, and $\hat{H}_{1'1}^c=\hat{H}_{11'}^c$ by an independent Gaussian ensemble $(\mathrm{GOE})_A$, the variance of the matrix elements of which is fixed through Eq. (30) by the flux Φ exchanged between $\mathcal{R}_1$ and $\mathcal{R}_1{}'$. Because, however, there are no null matrix elements due to P, and using the very same reasoning leading to Eq. (5.29) of [10], g should here be replaced by $g/2$ in Eq. (30) (using in the definition of the transition parameter Λ the mean spacing of a given symmetry class).

Turning now to the symmetric basis $[\Psi_\pm^r=(\Psi_1^r\pm\Psi_1^{r\prime})/\sqrt{2}, |\pm,\alpha\rangle=(|1,\alpha\rangle\pm|1',\alpha\rangle)/\sqrt{2}]$, the Hamiltonian matrix in the $+$ or $-$ symmetry class is modeled as

$$\hat{H}_\pm\begin{pmatrix}\Psi_\pm^r\\ \mathcal{E}_\pm^c\end{pmatrix}=\begin{pmatrix}E^r & \{v\}\\ \{v\} & (\mathrm{GOE})_D\pm(\mathrm{GOE})_A(\Phi)\end{pmatrix}\begin{pmatrix}\Psi_\pm^r\\ \mathcal{E}_\pm^c\end{pmatrix}. \tag{B3}$$

If the barrier between $\mathcal{R}_1$ and $\mathcal{R}_1{}'$ is ineffective, the matrix elements of $(\mathrm{GOE})_D$ and $(\mathrm{GOE})_A$ have the same variance, so that their sum and difference are decorrelated. We recover in this way that if all regions are symmetric by P, there is no correlation between the different symmetry classes. On the other hand, if the partial barrier is effective [i.e., if the transition parameter Λ_A associated with $(\mathrm{GOE})_A$ is much smaller than one], $\hat{H}_+$ and $\hat{H}_-$ are actually correlated. To be more precise, if one first diagonalizes the chaotic part of $\hat{H}_+$ and $\hat{H}_-$, the chaotic levels will appear extremely correlated if looked at a scale larger than $\Lambda_A^{1/2}$, but essentially decorrelated on a range smaller than $\Lambda_A^{1/2}$.

2. Ensembles Eqs. (32) and (33)

The construction of the ensemble Eq. (32) is slightly more involved than either of the two above "pure cases" since the corresponding classical transport configuration contains some regions which are symmetric by P and some which are not. One can, however, proceed in essentially the same way as for the ensemble Eq. (B3), working in a basis "relevant" to the classical configuration displayed in Fig. 9. The point here is that, although the region $\mathcal{R}_2$ is invariant by P, the simplest way to take into account this symmetry is to suppose that the set of vectors "semiclassically" belonging to $\mathcal{R}_2$ are shared in two subsets $\{|2,\beta\rangle\}$ and $\{|2',\beta'\rangle\}$ $(\beta,\beta'=1,2,\ldots)$ such that $|2',\beta\rangle=P|2,\beta\rangle$. Noting $\mathcal{E}^c$ the Hilbert subspace generated by $(|1,\alpha\rangle,|2,\beta\rangle)$ and $\mathcal{E}^{c\prime}$ the one generated by $(|1',\alpha'\rangle,|2',\beta'\rangle)$, the Hamiltonian matrix takes as above the form

$$\hat{H}\begin{pmatrix}\mathcal{E}^c\\ \mathcal{E}^{c\prime}\end{pmatrix}=\begin{pmatrix}\hat{H}_D & \hat{H}_A\\ \hat{H}_A & \hat{H}_D\end{pmatrix}\begin{pmatrix}\mathcal{E}^c\\ \mathcal{E}^{c\prime}\end{pmatrix}, \tag{B4}$$

where using the same way of reasoning, $\hat{H}_D$ and $\hat{H}_A$ can be modeled by the ensembles

$$\hat{H}_D\begin{pmatrix}\Psi^r\\ \mathcal{E}_1^c\\ \mathcal{E}_2^c\end{pmatrix}=\begin{pmatrix}E^r & \{v\} & 0\\ \{v\} & (\mathrm{GOE})_1 & \Lambda_{12}^D\\ 0 & \Lambda_{12}^D & (\mathrm{GOE})_2^D\end{pmatrix}\begin{pmatrix}\Psi^r\\ \mathcal{E}_1^c\\ \mathcal{E}_2^c\end{pmatrix}, \tag{B5}$$

$$\hat{H}_A\begin{pmatrix}\Psi^r\\ \mathcal{E}_1^c\\ \mathcal{E}_2^c\end{pmatrix}=\begin{pmatrix}0 & 0 & 0\\ 0 & 0 & \Lambda_{12}^A\\ 0 & \Lambda_{12}^A & (\mathrm{GOE})_2^A\end{pmatrix}\begin{pmatrix}\Psi^r\\ \mathcal{E}_1^c\\ \mathcal{E}_2^c\end{pmatrix}. \tag{B6}$$

Disregarding for a moment what fixes the value of the variance of the matrix elements in the different blocks, we simply stress that since the $(|2,\beta\rangle)$ and $(|2',\beta'\rangle)$ semiclassically belong to the same classical region $\mathcal{R}_2$, the variances are the same for $(\mathrm{GOE})_2^D$ and $(\mathrm{GOE})_2^A$, and for the same reason $\Lambda_{12}^D=\Lambda_{12}^A$.

Going to the symmetric basis, one obtains as usual

$$\hat{H}_\pm=\hat{H}_D\pm\hat{H}_A, \tag{B7}$$

which, using the fact that the sum and difference of two independent Gaussian distributions are independent Gaussian distributions, leads to

$$\hat{H}_\pm=\begin{pmatrix}E^r & \{v\} & 0\\ \{v\} & (\mathrm{GOE})_1 & \Lambda_{12}^\pm\\ 0 & \Lambda_{12}^\pm & (\mathrm{GOE})_2^\pm\end{pmatrix}. \tag{B8}$$

Because, as compared to the ensemble Eq. (B1), only the correlation between the symmetry class has been changed here, the variance of the matrix elements in the different blocks is the same. [This can be checked directly by counting the number of nonzero matrix elements in Eqs. (B5) and (B6).] In particular $\Lambda_{12}^\pm$ is related to the flux Φ_{12} through Eq. (30) (no factor 2 here). We therefore obtain the ensemble Eq. (32) (except that, since taking Λ_{12} the same or not in the two symmetry classes does not change the resulting distributions, we omitted the $\pm$ in this latter equation).

To conclude, let us stress that the above construction can be generalized in a straightforward way for any classical transport configuration containing both symmetric and nonsymmetric chaotic subregions, provided there is no direct communication between a region and its symmetric partner in the latter case. Under this condition,

one obtains that the variance of the matrix elements in the different blocks is the one given by the prescriptions derived in [10] and the diagonal GOE blocks should be taken as the same in the two symmetry classes if the corresponding region is not invariant by P, and as uncorrelated in the other case. The ensemble Eq. (33) is obtained in this way with the additional classical structure.

[1] M. Wilkinson, Physica **21D**, 341 (1986).

[2] A.M. Ozorio de Almeida, J. Phys. Chem. **88**, 6139 (1984).

[3] A. Einstein, Verh. Deutsch. Phys. Ges. Berlin **19**, 82 (1917) [English translation by C. Jaffe, JILA Report No. 116 (unpublished)]; L. Brillouin, J. Phys. Radium **7**, 353 (1926); J.B. Keller, Ann. Phys. (N.Y.) **4**, 180 (1958).

[4] A.N. Kolmogoroff, Dokl. Akad. Nauk. SSSR **98**, 527 (1954); V.I. Arnold, Usp. Mat. Nauk. SSSR **18**, 13 (1963); J. Moser, Nachr. Akad. Wiss. Göttingen **1** (1962).

[5] V.I. Arnold, *Mathematical Methods of Classical Mechanics* (Springer-Verlag, New York, 1978).

[6] V.P. Maslov and M.V. Fedoriuk, *Semiclassical Approximation in Quantum Mechanics* (Reidel, Dordrecht, 1981) [original Russian edition 1965].

[7] M.J. Davis and E.J. Heller, J. Chem. Phys. **75**, 246 (1981).

[8] Just to give two examples, for the water molecule see R. T. Lawton and M. S. Child, Mol. Phys. **37** (1979) 1799; and for benzophenone, E. J. Heller, in *Chaos et Physique Quantique / Chaos and Quantum Physics*, Proceedings of Les Houches Summer School, Session LII, 1989, edited by M.J. Giannoni, A. Voros, and J. Zinn-Justin (North-Holland, Amsterdam, 1991).

[9] W.A. Lin and L.E. Ballentine, Phys. Rev. Lett. **65**, 2927 (1990); Phys. Rev. A **45**, 3637 (1992); F. Grossmann, T. Dittrich, P. Jung, and P. Hänggi, Phys. Rev. Lett. **67**, 516 (1991); J. Stat. Phys. **70**, 229 (1993); R. Utermann, T. Dittrich and P. Hänggi (unpublished).

[10] O. Bohigas, S. Tomsovic, and D. Ullmo, Phys. Rep. **223** (2), 45 (1993).

[11] O. Bohigas, D. Boosé, R. Egydio de Carvalho, and V. Marvulle, Nucl. Phys. **A560**, 197 (1993).

[12] R. E. Langer, Phys. Rev. **51**, 669 (1937).

[13] B. Lauritzen, Phys. Rev. A **43**, 603 (1991).

[14] O. Bohigas, S. Tomsovic, and D. Ullmo, Phys. Rev. Lett. **64**, 1479 (1990).

[15] M. Wilkinson, J. Phys. A **20**, 635 (1987).

[16] M.C. Gutzwiller, *Chaos in Classical and Quantum Mechanics* (Springer-Verlag, New York, 1990); P. Cvitanovič and B. Eckhardt, Phys. Rev. Lett. **63**, 823 (1989); M.V. Berry and J.P. Keating, J. Phys. A **23**, 4839 (1990); G. Tanner, P. Scherer, E.B. Bogomolny, B. Eckhardt, and D. Wintgen, Phys. Rev. Lett. **67**, 2410 (1991); R. Aurich, C. Mathies, M. Sieber, and F. Steiner, *ibid.* **68**, 1629 (1992).

[17] A. Voros, J. Phys. A **21**, 685 (1988); M.-A. Sepúlveda, S. Tomsovic, and E.J. Heller, Phys. Rev. Lett. **69**, 402 (1992).

[18] S. Tomsovic and E.J. Heller, Phys. Rev. Lett. **70**, 1405 (1993).

[19] O. Bohigas, in *Chaos et Physique Quantique / Chaos and Quantum Physics* (Ref. [8]).

[20] O. Bohigas, S. Tomsovic, and D. Ullmo, Phys. Rev. Lett. **65**, 5 (1990).

[21] S. Tomsovic, Doctoral dissertation, University of Rochester, 1986.

[22] J. B. French, V.K.B. Kota, A. Pandey, and S. Tomsovic, Ann. Phys. (N.Y.) **181**, 198 (1988).

[23] T.A. Brody, J. Flores, J.B. French, P.A. Mello, A. Pandey, and S.S.M. Wong, Rev. Mod. Phys. **53** (3), 385 (1981).

[24] S. Aubry and P.Y. Le Daeron, Physica **8D**, 381 (1983).

[25] R.S. MacKay, J.D. Meiss, and I.C. Percival, Phys. Rev. Lett. **52**, 697 (1984); Physica **13D**, 55 (1984); **27D**, 1 (1987).

[26] M.J. Davis, J. Chem. Phys. **83**, 1016 (1985); M.J. Davis and S.T. Gray, *ibid.* **84**, 5389 (1986); S.T. Gray, S.A. Rice, and M.J. Davis, J. Phys. Chem. **90**, 3470 (1986); L.L. Gibson, G.C. Schatz, M.A. Ratner, and M.J. Davis, J. Chem. Phys. **86**, 3263 (1987).

[27] R.C. Brown and R.E. Wyatt, Phys. Rev. Lett. **57**, 1 (1986).

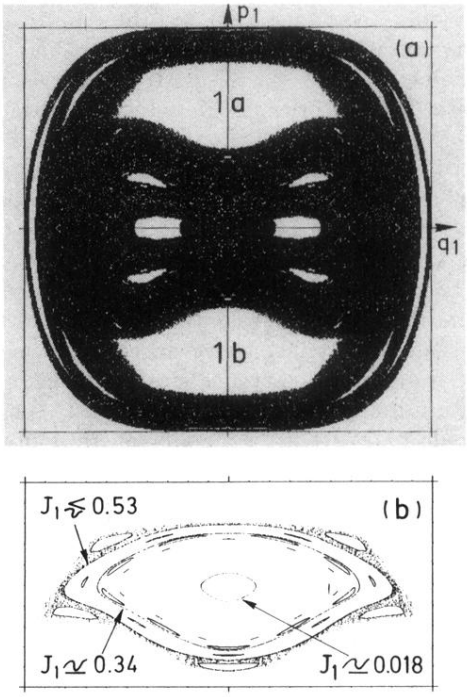

FIG. 2. (a) $q_2 = 0$ surface of section for $\{(\lambda, b) = (-0.25, \pi/4)\}$. The blackened region is a single connected zone of chaotic motion. The KAM regions are the open areas. The large islands, denoted $1a$ and $1b$, are part of a 1:1 resonance island chain and are symmetric versions of each other. (b) The island $1a$ magnified. Included are the tori with (at $E = 1$) $J_1 = 0.018$ (the smallest to quantize in our spectrum), $J_1 = 0.34$, and $J_1 = 0.53$; see Fig. 4.

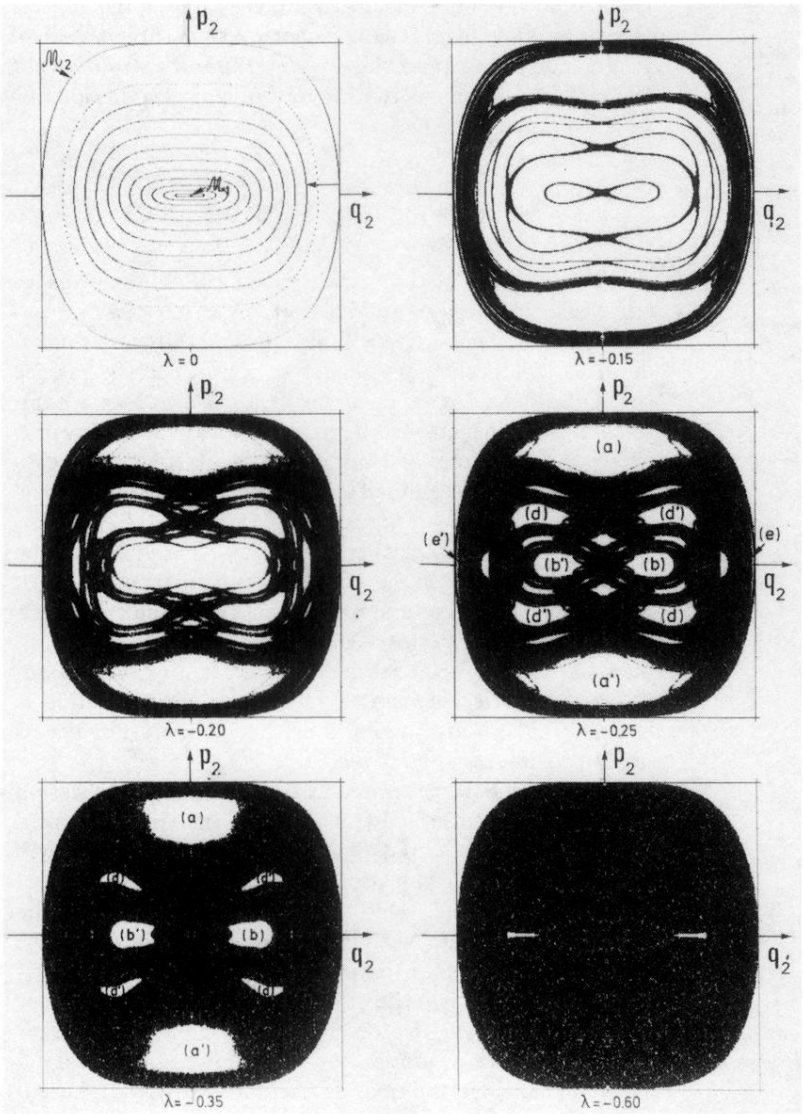

FIG. 5. $q_1 = 0$ surface of sections showing the changing dynamics with λ ($b = \pi/4$). The system becomes increasingly chaotic as λ decreases. Also given in Ref. [10].